Mineralogy and geochemistry of sulfide ores in ocean-floor hydrothermal fields associated with serpentinite protrusions

A. Yu. Lein[1], N. V. Ulyanova[1], A. A. Ulyanov[2], G. A. Cherkashev[3] and
T. V. Stepanova[3]

[1]Shirshov Institute of Oceanology, Russian Academy of Sciences
[2]Lomonosov Moscow State University
[3]All-Russia Institute of Oceanology (VNIIOkeangeologiya)

Abstract. The aim of this paper is to analyze and compare the mineralogy and geochemistry of copper–zinc sulfide ores from the Logachev-2 and Rainbow hydrothermal fields of the Mid-Atlantic Ridge (MAR), confined to serpentinite protrusions. It was found that the Zn(Fe) and Cu, Fe(Zn) sulfides had been deposited in black smokers pipes almost simultaneously from intermittently flowing, nonequilibrium H_2S-low solutions of different temperatures. The Pb isotope composition confirmed that the source of lead had been the deep oceanic crust. The ores of the Rainbow Field contain 20-fold more Co than the ores restricted to the basalts and show a high ratio of Co/Ni = 46. The Rainbow ore is enriched in heavy ^{34}S isotope ($\delta^{34}S_{av} = 10^o/_{oo}$) because of the constant flow of cold sea water into the subsurface zone of the hydrothermal system. The ore of the Logachev-2 field is 8 times higher in gold compared to the other MAR regions. The sulfide ores of the Rainbow and Logachev-2 fields have no analogues among the MAR ore occurrences in terms of the enrichment in useful components (Zn, Cd, Co, and Au).

Introduction

Like the Logachev-1 hydrothermal field, the active Rainbow and Logachev-2 fields are located in the inner rift of the Mid-Atlantic Ridge (Figure 1). Their hydrothermal sulfide ore occurrences are associated with serpentinite and serpentinized ultramafic rocks rather than with oceanic basalts. It was on the Logachev-1 and Rainbow active fields that a principally new type of an ore-forming hydrothermal system, known as a deep-source system, was discovered in contrast to the widely known axial hydrothermal systems [*Bogdanov et al.,* 1995, 1997].

The Logachev-2 hydrothermal field was discovered in 1993–1994 during a cruise of the R/V Professor Logachev

on the eastern slope of the rift valley 5.5 km from the Logachev-1 field [*Cherkashev et al.,* 2000]. The coordinates of its center are $14°43.22' N$ and $44°56.27' W$, its area is 0.15×0.2 km^2 (Figure 2).

The Rainbow field (Figure 3) was discovered in 1997 [*Fouquet et al.,* 1997]. It was described extensively by Russian and foreign investigators [*Bogdanov et al.,* 1999, 2000; *Desbruyeres et al.,* 2000, 2001; *Lein et al.,* 2000; *Pimenov et al.,* 2000; *Simonov et al.,* 2000; *Vikentiev et al.,* 2000].

The Logachev-2 field is situated at a depth of ~2700 m, Rainbow at ~2300 m (Figure 1). Many investigators believe that the near-surface hydrothermal ore deposition on the Rainbow and Logachev-1 fields is accompanied by "the processes of phase separation, which leads to the instabilities in the temperature conditions and in the salt composition of the ore-forming fluids" [*Bogdanov et al.,* 1999].

At the same time, along with the common geological and geochemical situation (association with serpentinite intrusions and substantial variations in mineral composition), the hydrothermal products of the above mentioned fields have their own specific features which are the subject of this paper.
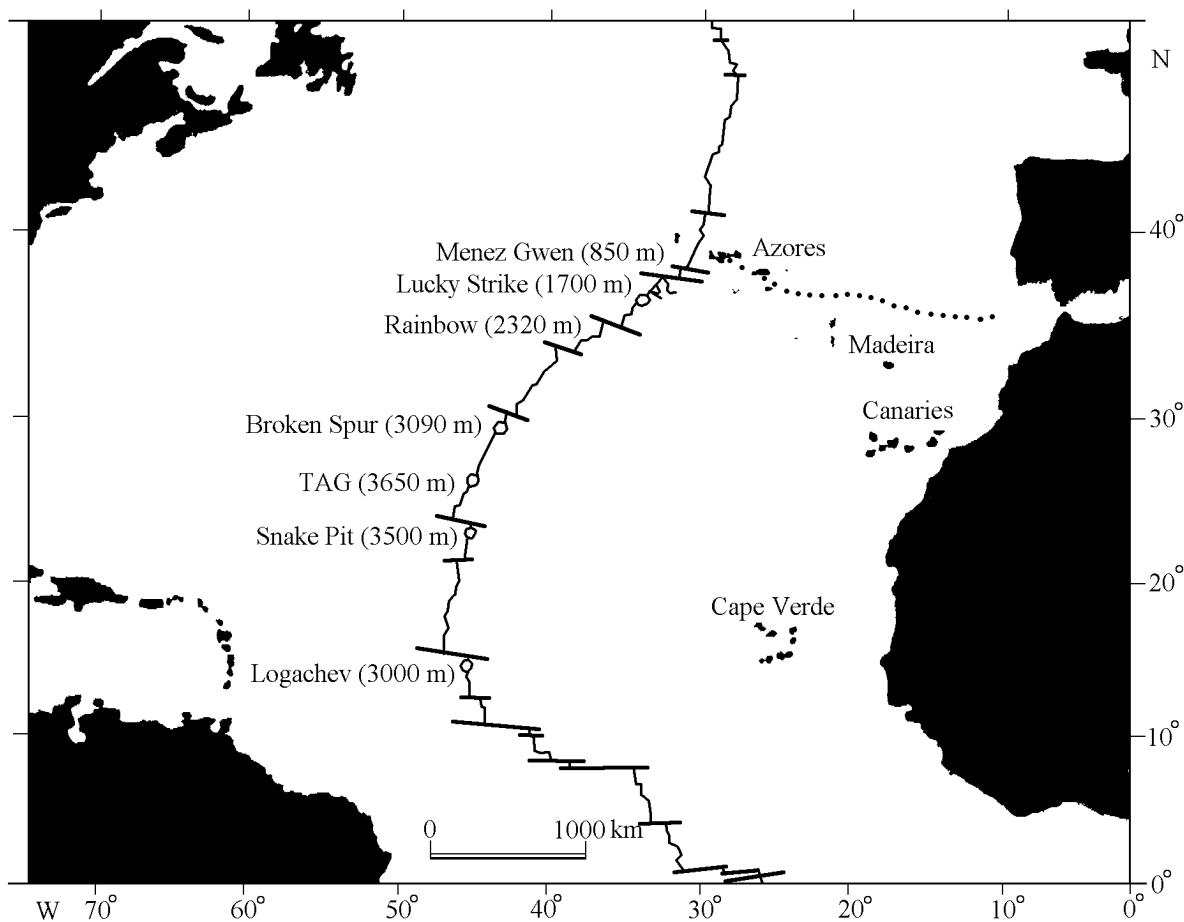
Figure 1. Schematic distribution of active hydrothermal fields on the Mid-Atlantic Ridge between the equator and the Azores Islands (after [*Desbruyeres et al.,* 2001]).

Ore Material and Methods of Study

On the Logachev-2 field we studied hydrothermal and sulfide ores collected by a remote grab sampler controlled from the R/V Professor Logachev in 1998 (Figure 2). We analyzed a large sample (120 kg), consisting of cone-shaped pipes grown together, collected from the near-top part of a large orebody (Site 384).

On the Rainbow field samples were collected using a Mir-1 submersible during cruise 42 of R/V Akademik Mstislav Keldysh in the autumn of 1999. Samples were collected from the older (Western) part of the field to the younger (Eastern) end of the field (Figure 3). We studied six sulfide pipes characterizing active and inactive structures.

The chemical compositions of the ores were determined in the laboratories of VNIIOkeangeologiya by atomic absorption and quantitative spectral methods. Detailed mineralogical analyses of the Rainbow hydrothermal ores were made after their cleaning in water using a UZDM-1 dispergator (22 and 35 kHz frequencies with an exposition time of 1–1.5 min). During the early stage of the work the specimens were studied under an MBS-9 binocular microscope and a

POLAM M-212 optical polarization microscope. After this preliminary diagnostics of the mineral phases each specimen was analyzed under a CAMSCAN scanning electron microscope with a Link-10000 energy-dispersion analyzer (analysts E. V. Guseva and N. N. Korotaeva, Moscow University). The resulting numerous photographs in back-scattered electrons (BSE) and the exact knowledge of the qualitative compositions of minerals contributed to the subsequent detailed study of the chemical composition variations of minerals on a Cameca SX-50 electron microprobe equipped with three wave spectrometers (analysts N. N. Kononkova and N. N. Korotaeva, Moscow University). Relationships among the minerals and the sequence of their deposition from the hydrothermal solutions were established from the optical study of the specimens in reflected light and from their study on a CAMSCAN instrument in back scattered electrons and from the images of the surfaces of artificial fractures in secondary electrons (SEI).

The results of our studies were based on 33 optical and 41 electron microscope photographs, and also on the 340 microprobe analyses of a great variety of mineral phases. In addition, the samples from the Rainbow and Logachev-2 fields were analyzed under an ABT-55 electron microscope with
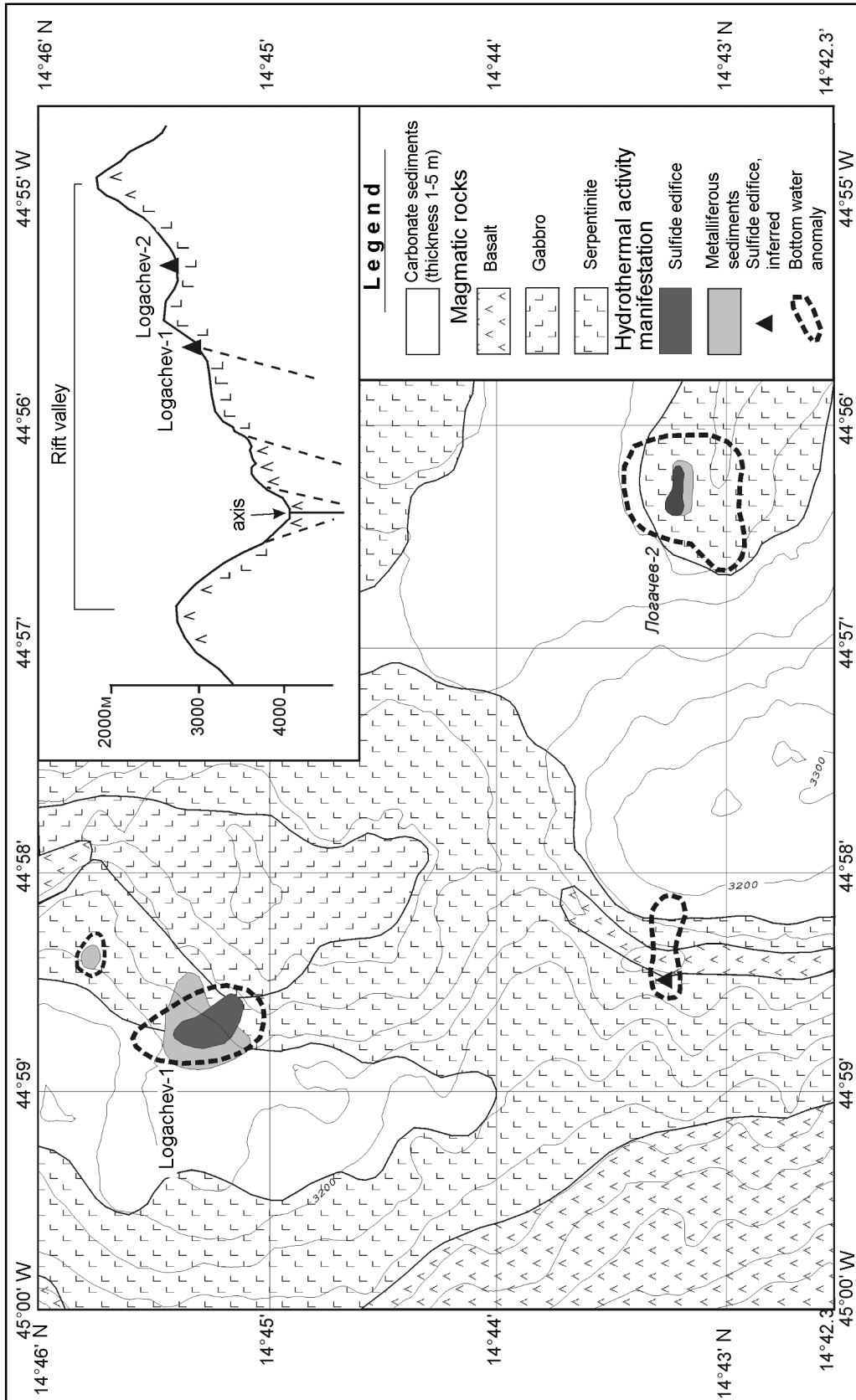
Figure 2. Schematic distribution of the Logachev-1 (active) and Logachev-2 (inactive) hydrothermal fields in map view and in geological section (inset map).
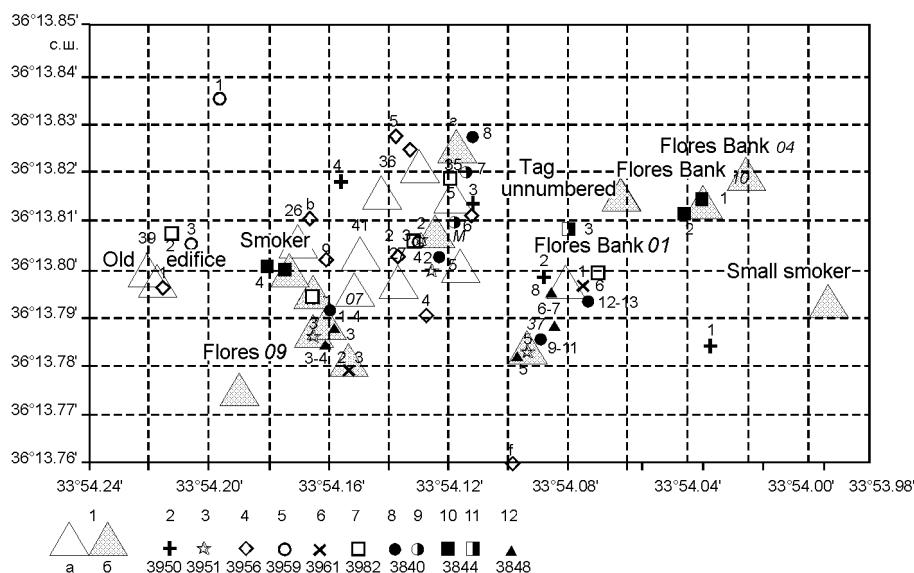
Figure 3. Schematic distribution of sulfide structures and the sites of sample collection on the Rainbow active hydrothermal field during cruises 41 and 42 of R/V Akademik Mstislav Keldysh: 1) hillocky hydrothermal structures: 1a – active, 1b – old inactive; 2–12) sites of collecting sulfide ore samples and the numbers of the diving sites of the MIR-1 and MIR-2 submersibles (after [*Sagalevich et al.*, 2000]).

a Link-10000 energy-dispersion analyzer at an acceleration voltage of 25 kV in the Institute of Precambrian Geology and Geochronology (analysts M. P. Pavlov and M. D. Tolmachev). The final results include only the elements, the contents of which exceeded the analytical error (2σ). The microprobe had a diameter of 3 μm.

Geological Situation

Logachev-2 hydrothermal field. Six orebodies were located there by teleprofiling. A relatively large orebody was outlined at a depth of 2670–2740 m. It is 140–150 m long and varies in width from 40 m in the east to 80 m in the west.

The height of the body is 10–12 m. It has a complex rough surface. Groups of inactive pipes, 0.5 to 0.6 m high, occur at the site where an ore sample was collected. Samples of soft hydrothermally altered rocks were raised from the center of this ore occurrence along with ore materials. Some 100–150 m south of this large ore body, five small isometric hill-shaped ore structures were discovered, ranging from 20 to 60 m in diameter and rising as high as 6 m. The age of the Logachev-2 sulfide deposit was estimated as 3.9±0.4 thousand years (Table 1).

Rainbow hydrothermal field is located on the western slope of the Rainbow Ridge which is an axial ridge of the rift strike. This axial ridge is a serpentinite protrusion [*Barriga et al.,* 1997]. The hydrothermal field is located on a relatively gently dipping ground (15°–20°) at a depth of 2270–2320 m. It is 250 m lone from west to east and 50 m long from north to

Table 1. Results of the radiochemical analyses of sulfide ore samples collected from the Rainbow (Site 3982) and Logachev-2 hydrothermal fields during cruise 42 of R/V Akademik Mstislav Keldysh

Sample no.	Mass	^{238}U ppm	^{238}U dpm	^{234}U dpm	$\frac{^{234}U}{^{238}U}$	^{232}Th dpm	^{230}Th dpm	$\frac{^{230}Th}{^{234}U}$	Age, thou. y.
Rainbow									
M1-3a	4.01	3.60±0.15	2.59±0.11	2.86±0.12	1.11±0.03	0.054±0.006	0.55±0.02	0.191±0.011	23.0±1.5
M1-4b	4.01	4.75±0.32	3.42±0.23	3.71±0.25	1.08±0.04	0.023±0.003	0.07±0.01	0.020±0.003	2.2±0.3
M1-2/5	4.11	0.06±0.01	0.044±0.004	0.050±0.004	1.13±0.14	b.e.e.	<0.009	<0.181	<22.0
M1-6	4.89	0.24±0.01	0.17±0.01	0.21±0.01	1.21±0.08	b.e.e.	0.007±0.001	0.035±0.005	3.9±0.6
Logachev-2									
384-4	4.55	3.37±0.27	2.43±0.20	2.54±0.20	1.05±0.05	0.001±0.001	0.09±0.01	0.035±0.004	3.9±0.4

Analyst V. Yu. Kuznetsov. BNIIGeografiya. St. Petersburg; b.e.e – below experimental error.

Table 2. Chemical compositions of ores from the MAR hydrothermal fields

	S	Fe	Zn	Cu	Pb	SiO$_2$	CaO	MgO	Al$_2$O$_3$	Cd	Co	Ni	As
	%									ppm			
Rainbow (n=9) (n=42)*	n.d.	28.99 24.43	23.66 23.39	7.88 10.52	0.04 0.05	1.46	1.48	1.09	0.28	800	4200 6100	89.4 18.8	163
Logachev-2 (n=5)	20.9	17.55	25.4	14.72	0.07	9.73	0.52	0.24	0.36	700	500	20	522
Logachev-1 (n)	25.11 (48)	21.8 (64)	2.86 (64)	28.02 (64)	0.036 (55)	4.9 (41)	8.38 (48)	1.19 (42)	1.27 (37)	60.2 (34)	409 (64)	149 (58)	370 44
Sulfides on MAR basalts (n=427)	34.06	30.75	5.21	9.64	0.033	12.1	1.51	0.4	0.25	190	200	29	270

	Ba	Au	Ag	Mn	Y	Ga	Ge	Zr	Ti	V	Cr	Bi	Sn
	ppm												
Rainbow (n=9)	687	3.1	361.9	<100	6.9	59.7	74.2	154.9	747.5	32.2	29	<0.5	>50
Logachev-2 (n=5)	<100	23.8	92	<100	5	43	50.4	98	772	15.6	20	26.6	≫50
Logachev-1 (n)	1494 (42)	9.61 (52)	50.9 (51)	271 (25)	n.d.	n.d.	n.d.	n.d.	732.8 (14)	n.d.	n.d.	n.d.	n.d.
Sulfides on MAR basalts (n=427)	790	3	77.2	483	7.4	41.2	39.2	53.5	220	19.7	24.3	2.2	20.9

Analyses were made in VNIIOkeangeologiya, those marked with * were made in the Institute of Oceanology, Russian Academy of Sciences, analyst N. M. Zavadskaya;
Fe, Zn, Cu, Pb, CaO, MgO, Cd, Co, and Ag were determined by atomic absorption;
SiO$_2$, Al$_2$O$_3$, and S, by wet chemical analysis;
Au, by spectrochemical analysis;
the other elements, by quantitative spectral analysis;
n.d. – not determined.

south (Figure 3). Ten large active and many inactive (relict) structures were found in this field. The ocen floor between them is made up of serpentinite, often covered by a layer of metalliferous sediments [*Bogdanov et al.,* 1999, 2000].

The age the sulfide mineralization ranges from 22–23 thousand years in the west (Table 1), where relict structures dominate, to 2.2–3.9 thousand years in the central presently active part of the field. Modern black smokers complicate the slopes of the high "active" hills and structures as individual and intricately intergrown pipes.

Results

Chemical Composition of Ores

The average chemical composition of the massive sulfide ores from the hydrothermal fields is given in Table 2. The major elements of the ores are S, Fe, Zn, and Cu. Geochemically the ores can be rank as copper–zinc ones controlled by a ratio between Cu and Zn. The contents of these elements vary greatly ranging from per cent fractions to 35 for Cu and are as high as 64% for Zn. The comparison of the bulk chemical compositions of ores from the Logachev-2 and Rainbow fields with the chemical compositions of ores from the oter MAR hydrothermal fields developed on the basalts suggests that the Logachev-2 and Rainbow ores are averagely 4–5 times higher in Zn (Table 2). Also characteristic of these ores are the high contents of Cd, Co, Ni, and some other elements, supposedly derived from ultramafic rocks (Table 2). The early studies of the Rainbow ores revealed the abnormally high contents of Co in them [*Lein and Sagalevich,* 2000; *Vikentiev et al.,* 2000]. The ore samples we analyzed showed the average Co concentration of 4200 ppm, which is 20 times as high as in all of the MAR ores associated with basalt volcanism, and 8–10 times higher than in the sulfides of the Logachev 1 and 2 fields (Table 2). The Co/Ni ratio in the Rainbow ores is the highest of all known MAR ores (∼46); this ratio is also relatively high in the Logachev-2 ores (∼25). The ores of both fields are distinguished by the eleveted concentrations of precious metals compared to the other known MAR ores. The ores of the Logachev-2 field
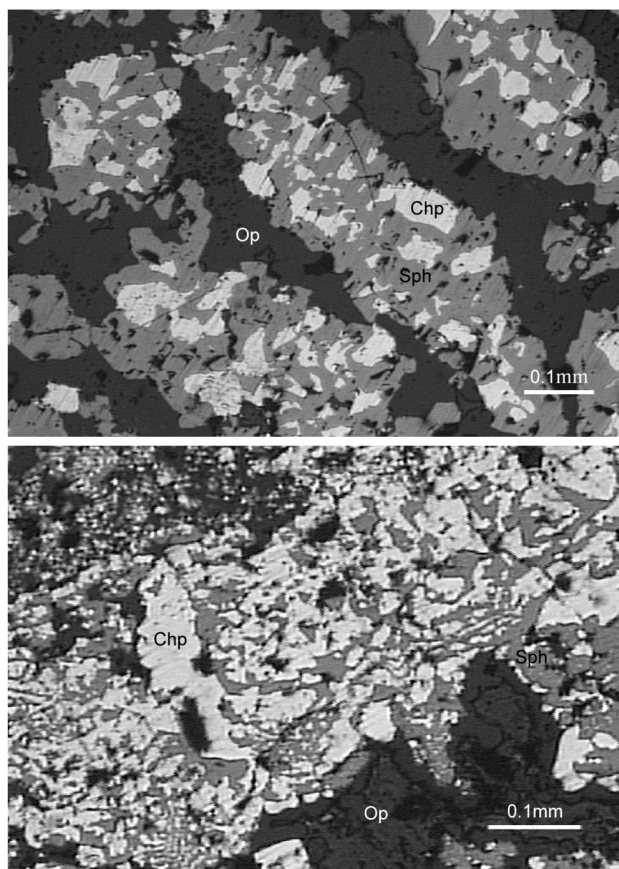
Figure 4. Relations among sphalerite (gray), Cu,Fe-sulfides (white), and silica minerals (dark gray) in the ores of the Logachev-2 field (Sample 384). Polished sections, reflected light.

showed gold concentrations (23.8 ppm) which are 3–8 times higher than those in the ores found on the basalts (Table 2).

The concentrations of gold in the Rainbow ores varies from 1 to 5 ppm (Table 2). The higher contents of gold (12 ppm) in the Rainbow ores were found by ICP-MS measurements earlier [*Vikentiev et al.,* 2000]. The concentration of gold grows in the series of sulfide–magnetite ore (0.04–0.24 ppm) → anhydritesulfide ore → significantly Zn ore → copperzinc ore → copper ore (0.8–12 ppm).

High silver contents were discovered in the ores of the Rainbow field (average 362 ppm, Table 2). Much lower silver contents (<6.6 ppm) were found in the copper-bearing ores of the Rainbow field [*Vikentiev et al.,* 2000]. Also reported in this paper were the elevated concentrations of platinum-group elements (Pd, Pt, Ru, Rh) in the Rainbow ores.

To sum up, the sulfide ores of the Logachev-2 and Rainbow hydrothermal fields, spacially confined to serpentinite massifs, can be ranked, in in terms of the contents of Zn, Cd, Co and precious metals (Au, Ag, and others), as the richest ore formations of the ocean.

Mineral Composition of Ores

Logachev-2 field. The known pipes have a zonal structure expressed in the substitution of the predominant chalcopyrite mineralization in the near-conduit zone by sphalerite mineralization in the outer zone. The central pipe portions are characterized by close "graphic" growths of chalcopyrite and sphalerite and their rhythmic alternation (Figure 4), both suggesting their simultaneous formation, Sphalerite is represented by its ferrous variety (Table 3). The amount of opal growing over the sulfides may be as large as 10% (Figure 4). Single samples showed the partial replacement of chalcopyrite by chalcocite. Bornite and covellite can be found occasionally.

There are abundant gold grains. Microscopic grains of gold amd electrum, <5 microns in size, were found in cryptocrystalline quartz (Figure 5a, b, d, f), in its intergrowths with sphalerite (Figure 6b) and in chalcopyrite in its intergrowths with sphalerite (Figure 5e). The content of gold varies widely (Table 4) from 88 to 60 wt.%. Taking the contact between gold and electrum to be marked by 30 wt.% silver, most of the grains analyzed fall into the field of gold. There are also small amounts of copper (<6 wt.%) and iron (<2 wt.%). Zinc was often found in gold grains, its form being controlled by sphalerite ingrowths, which was confirmed by finding sulfur in them.

To sum up, gold is mainly restricted to siliceous minerals, which occupy the interstitial spaces beyween the sulfides (chalcopyrite and sphalerite), and seems to be the last crystallizing phase. The presence of zinc testifies to a close paragenetic relation with sphalerite. The purity of gold, determined by the formula $1000 \, Au/(Au+Ag)$, varies from 900 to 620, depending on the temperature of its crystallization and largely on pH and Eh. Great variations in gold purity are known to be caused by pH and Eh changes and also by the addition of silver [*Petrovskaya,* 1989]. The native gold of this field differs from the gold of the Logachev-1 field [*Lazareva et al.,* 1997] by its higher silver and zinc contents (Table 4). In this respect this gold is close to the native gold of the Mir structure (TAG field) sitting in basalts [*Borodaev et al.,* 2000; *Mozgova et al.,* 1998].

Along with native gold, the ores contain rare minerals, such as cobaltite, arsenides of a loellingite–safflorite series (Lazareva L. I., personal communication), galena, and sul-

Table 3. Compositions and formulas of sphalerite from the Logachev-2 hydrothermal field (from microprobe analyses, wt.%)

Analysis*	Zn	Fe	Cu	S	Formula
1	58.55	8.04	0.37	32.58	$(Zn_{0.86}Fe_{0.13}Cu_{0.01})_{1.00}S$
2	57.47	5.56	2.81	32.14	$(Zn_{0.86}Fe_{0.10}Cu_{0.04})_{1.00}S$
3	54.75	9.11	–	31.25	$(Zn_{0.83}Fe_{0.17})_{1.00}S$
4	45.52	11.02	8.62	34.85	$(Zn_{0.71}Fe_{0.17}Cu_{0.12})_{1.00}S$

*1–3 – polished sections, 4 – disk of a crushed material enriched in heavy liquid.
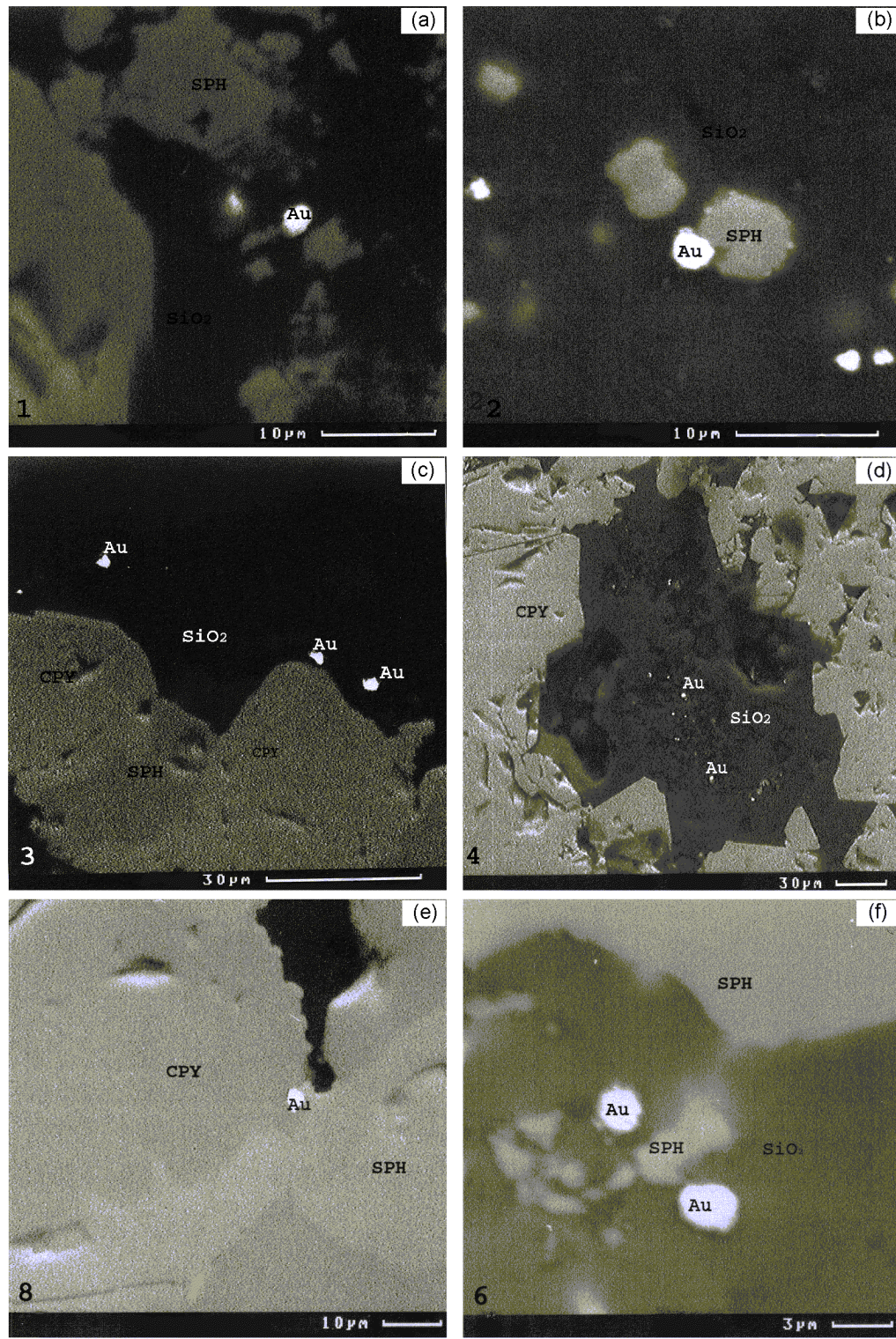
Figure 5. Relations of gold phases (Au) with the host minerals (Sample 384-2). Logachev-2 field.
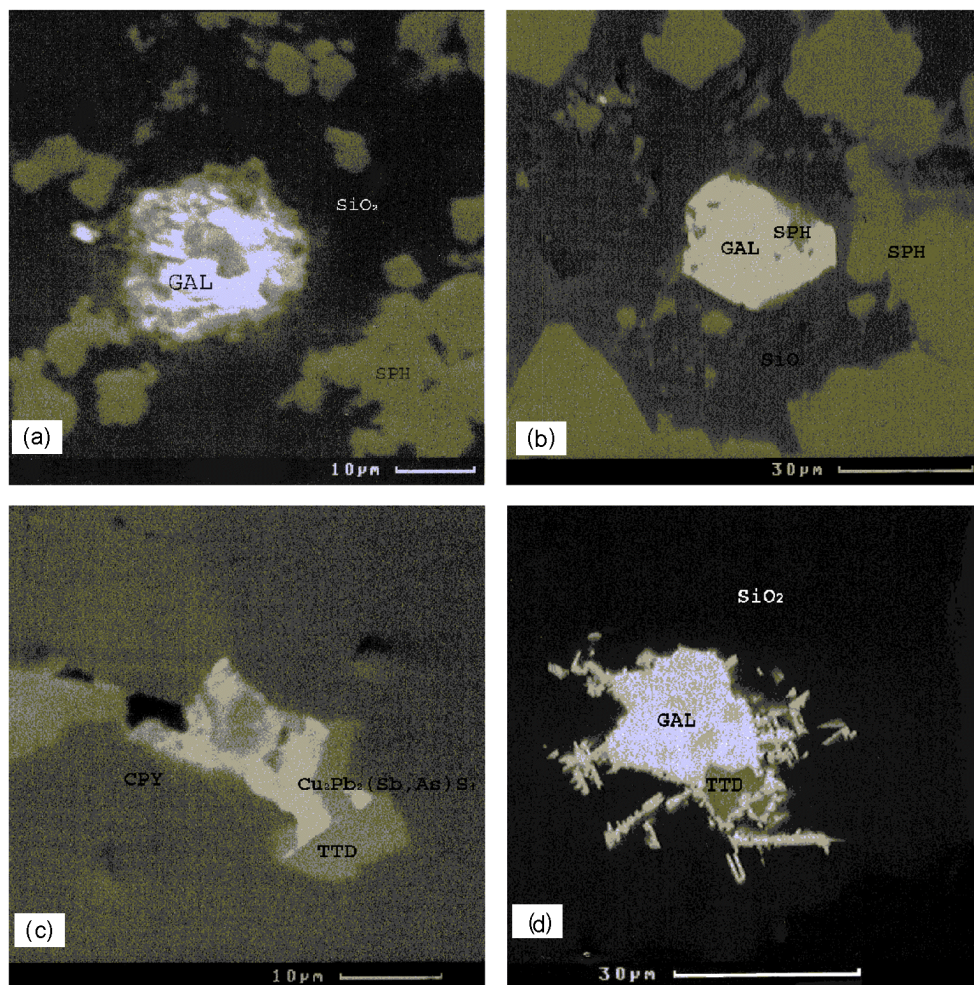
Figure 6. Morphology of galena (Gal) and sulfosalt (TTD-tetrahedrite and $Cu_3Pb_2[Sb, As]S_4$) in reflected electrons.

fosalts (Figure 6, Tables 5 and 6). A distinctive feature is an almost complete absence of iron disulfides and the abundance of crusts, the main minerals of which are goethite and hydrogoethite, less common being atacamite, limonite, opal, and manganese oxides and hydroxides.

In contrast to the ores of the Logachev-1 field, the Logachev-2 ores are dominated by sphalerite (average Zn = 25.4%) with very high gold concentrations (Au_{av} = 23.8 ppm) and comparatively high lead concentrations (Pb_{av} = 0.07%). In addition, elevated concentrations of bismuth and tin were found (Table 2).

Rainbow field. We analyzed ore samples collected from black smoker pipes (Figure 7). As a rule, the pipes have an indistinct zonal structure around the solution feeder. In some cases the feeder was found to be still hollow, but more often it is healed by the minerals of later assemblages. In most of the samples the metallic components included simultaneously sphalerite and copper-bearing minerals, the most abundant being isocubanite, chalcopyrite, and solid solutions based on cubanite and a $CuFe_3S_4$ phase (Table 2, Figures 8 and 9). There are also small amounts of pyrrhotite and pyrite (Figure 8g). No any additional ore mineral phases, except Cu- and Fe-sulfides and sphalerite, were found in some samples, for example, in 3982-M1-6 and 3983-M2-2/2. Complex relations between sphalerite and copper-bearing minerals in the Rainbow ores (Figures 8, 9) suggest an almost simultaneous precipitation of most of them from solutions of different temperatures and compositions. The most common of nonsulfide minerals are iron hydroxides (Figure 8) from the ocherous crusts covering the pipe walls, anhydrite, and silica minerals. Barite, aragonite, and magnetite were found occasionally.

Sphalerite is the main mineral of the ore samples collected on the Rainbow field. A sample from the 3982 M1-2 pipe showed a wide variation of the sphalerite composition: <1 to 20 mol.% FeS (Table 7, Figure 10), though not any regular trend was found in the variation of the Fe content in the vertical section of the structure.

Of interest is a positive correlation between the Fe and Co contents (Figure 11) and the almost complete absence of Ni. The maximum measured Ni content in sphalerite was found
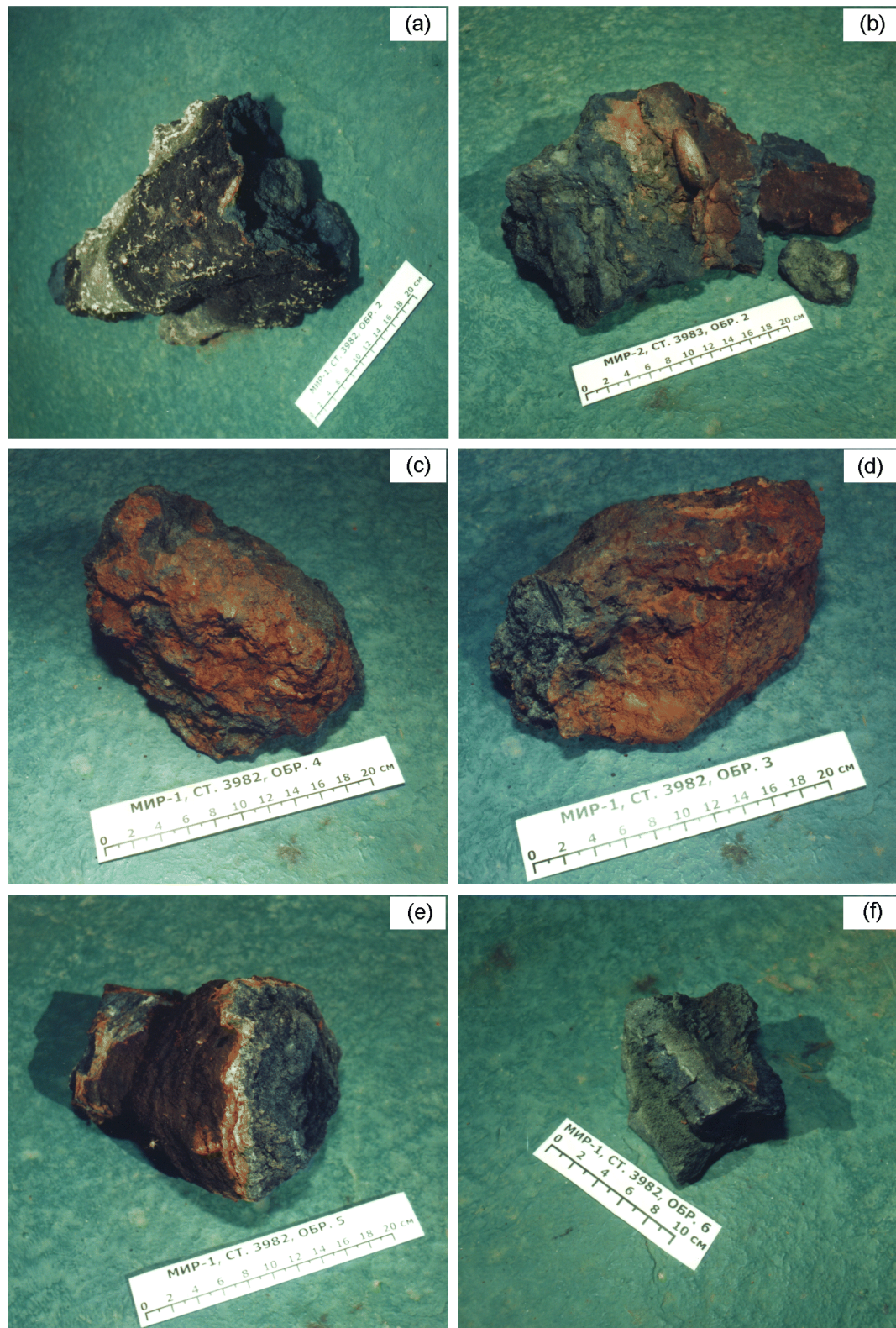
Figure 7. Ore samples from the Rainbow field: the cone-shaped peak of an old black smoker with sestonophages (white) on the surfaces (a) and with an adherent mussel shell (b); fragments of sulfide ore from a rock waste on the rock surface (c, d); fragments of black smoker pipes (e, f).
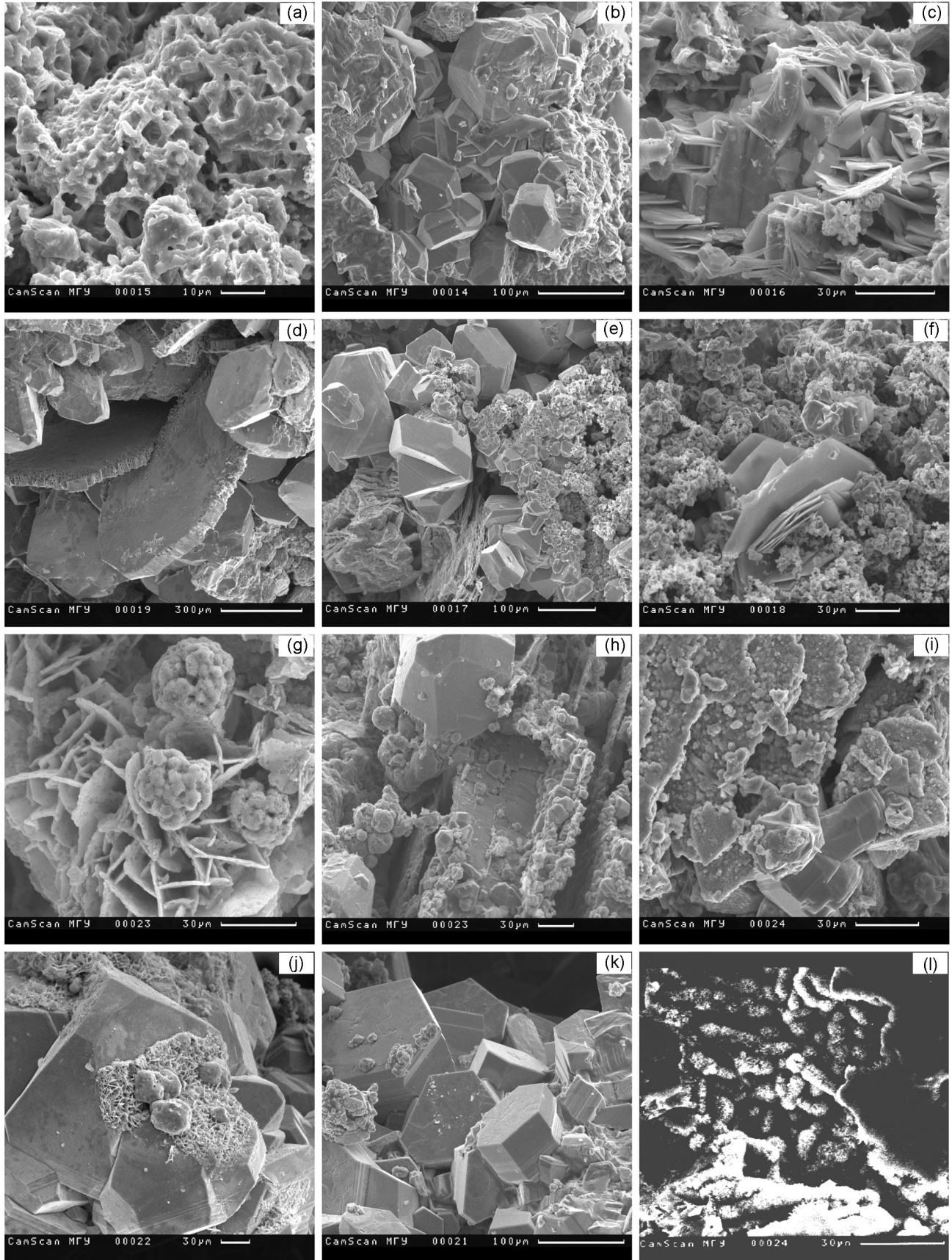
Table 4. Analyses of individual phases of gold–silver solid solutions (+ Zn, Cu) in sulfide ores from Logachev-2 hydrothermal field (wt.%)

Analysis*	Au	Ag	Zn	Cu	Fe	$\sum$	Formula
1	70.6	28.3	–	2.0	–	100.9	$(Au_{0.55}Ag_{0.41}Cu_{0.04})_{1.00}$
2	76.1	21.9	–	1.8	–	99.8	$(Au_{0.63}Ag_{0.32}Cu_{0.05})_{1.00}$
3	88.4	10.4	–	1.2	–	100.0	$(Au_{0.79}Ag_{0.18}Cu_{0.03})_{1.00}$
4	85.6	8.2	1.6	4.2	–	99.6	$(Au_{0.73}Ag_{0.13}Zn_{0.03}Cu_{0.11})_{1.00}$
5	76.8	19.7	3.6	–	–	100.1	$(Au_{0.62}Ag_{0.28}Zn_{0.10})_{1.00}$
6	81.1	12.8	–	6.1	–	100.0	$(Au_{0.65}Ag_{0.19}Cu_{0.16})_{1.00}$
7	60.9	32.1	2.9	2.2	2.1	100.2	$(Au_{0.46}Ag_{0.44}Zn_{0.06}Cu_{0.04})_{1.00}$
8	78.6	15.5	5.2	0.8	–	100.1	$(Au_{0.63}Ag_{0.22}Zn_{0.12}Cu_{0.03})_{1.00}$
9	81.6	12.6	1.1	5.0	–	100.3	$(Au_{0.78}Ag_{0.12}Zn_{0.02}Cu_{0.08})_{1.00}$

1–8 – polished sections, 9 – disk of a crushed material enriched in heavy liquid.

to be 0.06 wt.%. The other samples showed the Ni content in sphalerite below experimental error (0.02 wt.%). Sphalerite (Sample 3982-M1-2/7) was not found to contain molybdenite with calculated formula $Mo_{0.86}Zn_{0.10}S_{2.0}$. Taking the other sulfides, only sphalerite alone showed a relatively high Cl content: the mean value was found to be 0.13 (for N = 57), the maximum, 1.01 wt.%, possibly being a structural admixture.

Fe-sulfides. Pyrite and marcasite are relatively rare minerals in the Rainbow field. Pyrite was found only in the samples from the M1-3 and M1-4 structures (Table 8). Its composition is close to that of stoichiometric FeS_2. The minor elements of the ores are Cu (<0.6 wt.%), Zn (<0.4 wt.%), Au (<0.2 wt.%), Co (<0.15 wt.%), and Ag (<0.1 wt.%). One sample from the M1-4a structure was found to contain pyrrhotite $Fe_{0.87}S$, containing ~0.2 wt.% Co.

Cu- and Fe-sulfides. The compositional variations of the Cu,Fe-sulfides from the core of the 3982-M1-2 structure are plotted on a Fe vs Cu diagram (Figure 12) and listed in Table 7. Almost all of the analytical points reside on a FeS–CuS mixing line (some displacement of the points toward the origin was caused by the presence of Zn (<0.1 to 3.5 at.%) and produce a continuous trend of 2.7FeS·CuS, via cubanite ($CuFe_2S_3$), to almost stoichiometric chalcopyrite ($CuFeS_2$). It follows from Figure 12 that the core of the 3982-M1-2 structure has a poorly expressed vertical zoning

Table 5. Composition of galena from the Logachev-2 hydrothermal field (from microprobe analysis, wt.%)

Analysis	Pb	Zn	Cu	Fe	Sb	Se	S	$\sum$	Formula*
1	74.1	4.4	0.6	–	3.0	3.3	12.2	97.6	$Pb_{0.87}Zn_{0.16}Cu_{0.02}Sb_{0.06}(S_{0.90}Se_{0.10})_{1.00}$
2	82.2	1.9	–	–	–	6.3	9.2	99.6	$Pb_{1.07}Zn_{0.08}(S_{0.78}Se_{0.22})_{1.00}$
3	77.6	5.4	0.4	0.6	–	6.0	10.0	100.0	$Pb_{1.07}Zn_{0.23}Cu_{0.02}(S_{0.88}Se_{0.12})_{1.00}$
4	80.2	3.2	0.3	0.2	–	5.6	10.3	99.8	$Pb_{0.99}Zn_{0.12}Cu_{0.01}(S_{0.82}Se_{0.18})_{1.00}$
5	80.4	6.2	–	0.4	–	3.6	13.4	104.0	$Pb_{0.85}Zn_{0.21}Fe_{0.02}(S_{0.91}Se_{0.09})_{1.00}$

* Formula calculated for one (S+Se) atom.

Figure 8. Morphology of sulfide minerals: a – mineral aggregates of the Fe, Cu, Zn, and S composition from the top of an old structure (Sample 3982-M1-2/1); b – sphalerite crystals from a cavity in a finely dispersed matrix, a combination of sphalerite tetrahedrons and octahedrons, twin crystals (Sample 3982-M1-2/1); c – scaly crystals of a Fe, Zn, S composition (same sample); d – combination of scaly sphalerite crystals and Fe sphalerite octahedrons from crystalline ore in the central (near-channel) zone of a pipe (Sample 3982-M1-2/3); e – sphalerite crystals of different forms and sizes with different iron contents. The large octahedrons contain less iron than the fine-grained matrix from the bottom of the pipe central zone (Sample 3982-M1-2/5); f – intergrowth of sphalerite scales with Cu, Fe, and Cr in the fine-grained matrix (Sample 3982-M1-2/5); g – intergrowth of sphalerite scales with pyrite framboids (Sample 3982-M1-3); h – relations between large sphalerite octahedrons and fine-grained sphalerite of the matrix (Sample 3982-M1-3); i – chalcopyrite and sphalerite intergrowths (Sample 3982-M1-4a); k – pyrite nodules on the scaly sphalerite complicating the faces of large sphalerite crystals (Sample 3982-M1-4c); l – large sphalerite crystals in intergrowths with fine-grained sphalerite (Sample 3982-M1-3a); m – bacteriogenic iron hydroxide material fron the outer surfaces of sulfide pipes (Sample 3982-M1-4c).
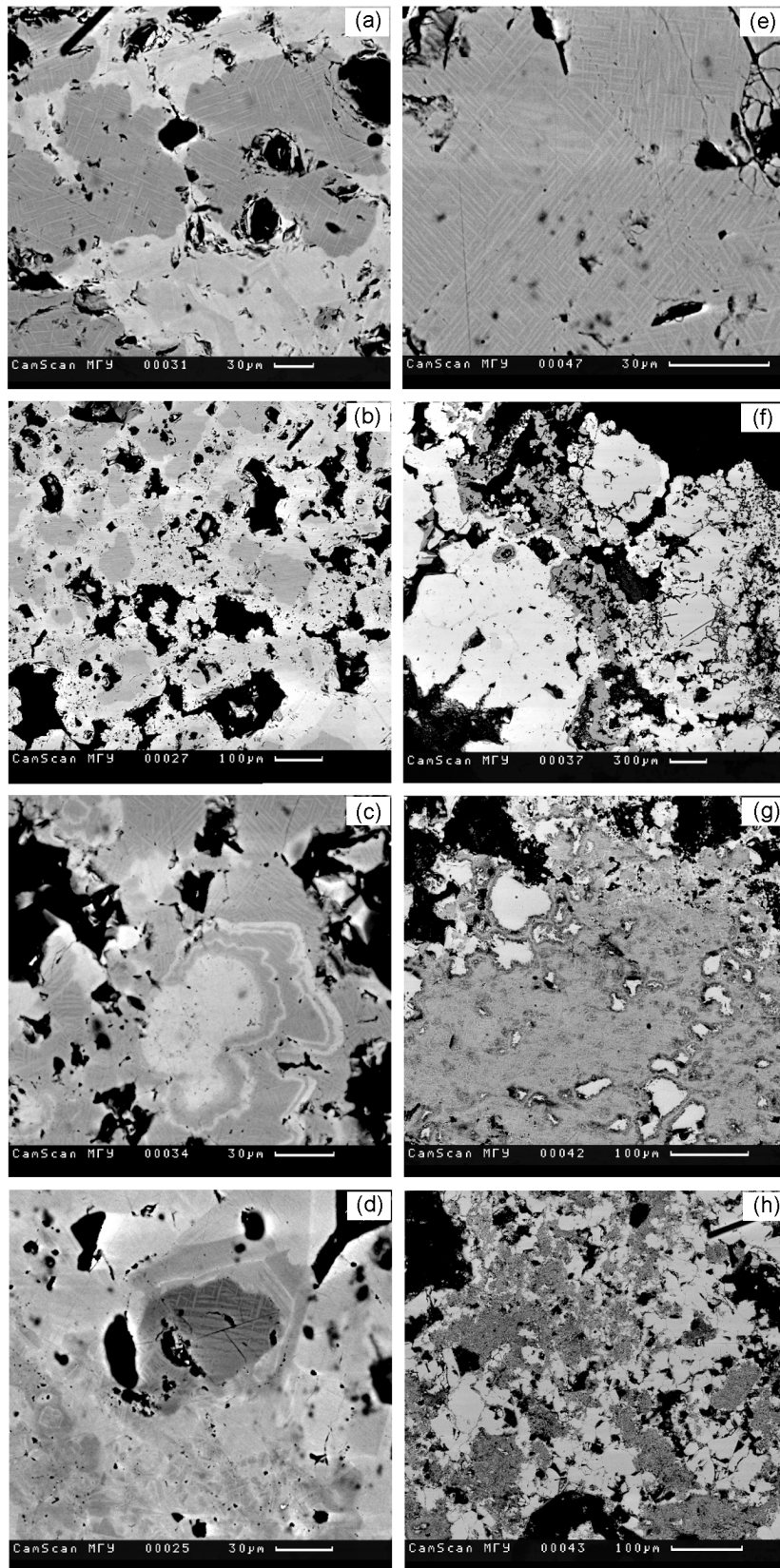
Table 6. Compositions of fahlore (1–2) and unnamed mineral (3) from microprobe analyses (wt.%)

Analysis	Cu	Sb	As	Fe	Zn	Pb	Te	S	$\sum$	Formula*
1	36.3	15.7	8.5	3.4	4.0	7.7	—	24.4	100.0	$Cu_{9.76}Fe_{1.04}Zn_{0.73}Pb_{0.63}(Sb_{2.20}As_{1.92})S_{13.00}$
2	37.2	21.8	5.3	5.8	2.8	—	2.9	23.3	99.1	$Cu_{10.24}Fe_{1.82}Zn_{0.75}(Sb_{3.13}As_{1.24})S_{13.00}$
3	17.8	8.2	4.4	3.8	1.4	46.9	—	15.6	98.1	

* Formula was calculated for 13 S atoms.

which was responsible for a decline of the FeS mole fraction in the monosulfide solid solution at the transition from the bottom to the top of the structure. In other words, the Cu/Fe ratio in the solution seems to have increased with the growth of the structure.

Bornite, chalcocite, covellite, and other Cu,Fe-sulfides are usually developed in the outer zones of the pipes, near the iron hydroxide crusts, and seem to be the products of the replacement of the primary generations of copper minerals (isocubanite and chalcopyrite). This process was accompanied by iron removal. Scarce small idiomorphic grains of magnetite and sulfotelluride (Sample 3982-M1-3a), having a composition of coloradoite ($Hg_{0.54}Cu_{0.20}Fe_{0.34}$)($Te_{0.56}S_{0.44}$), were found in association with Cu,Fe-sulfides.

Ag-rich mineral phases. Only three of the 340 sulfides analyzed showed the presence of Ag in the concentrations higher than 1 wt.%. It is of interest that these analyses produced a single linear trend on the Ag vs. Cl diagram (Figure 13), even though the atomic Ag/Cl ratio is variable

(8 to 23) and is considerably higher than the ratio Ag/Cl = 1 in kerargyrite (AgCl). We believe that this Ag/Cl correlation was produced during the analysis by the capture of the micrograins of native silver or Ag sulfides during the early phase of their replacement by cerargyrite.

Native gold with a minor admixture of silver (Table 9; Figure 14a, b) was found in a copper-type ore in Sample 4B in a ssociation with opal filling the interstices in isocubanite. The size of gold particles is ~3 microns.

Gold and platinum contents in sulfides. A relatively high Au content was found only in the Cu,Fe sulfides. (Figure 14a, b; Table 7). All sphalerite samples analyzed were found to contain gold in the amounts below the electron microprobe analytical error (0.05 wt.%).

Platinum was found in 7 out of 28 grains of Cu,Fe-sulfides that were analyzed for Pt (Table 10), that is, 25% of the Fe,Cu-sulfides contained Pt in the amounts above the ex-
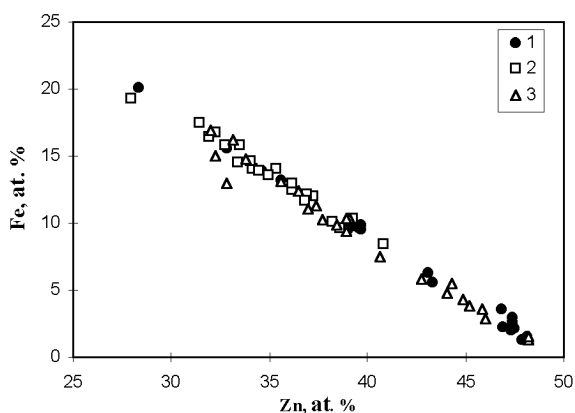

Figure 10. Variations of Fe content in sphalerite (Sample 3982-M1-2): 1 – top of the sample, 2 – middle, 3 – base.
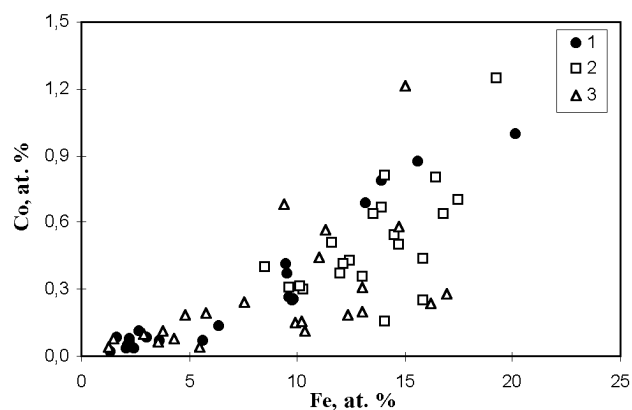

Figure 11. Positive correlation of Co and Fe contents in sphalerite (Sample 3982-M1-2): 1 – top of the sample (/1), 2 – middle (/3), 3 – base (/5).

Figure 9. Forms of various mineral phases in the Rainbow ores. Photograph in secondary electrons: a – fine-grained mass of a Cu, Fe, and S composition (dark) in sphalerite (Sample 3982-M1-2/3); b, c – zoned distribution of mineral phases: Cu, Fe, S (dark); Zn, Fe, S, and minor Cu (gray); Zn, Fe, S (light gray) (Sample 3983-M2-2/2); d – zoned pattern of sulfide phases: middle – reticulate isocubanite (dark) surrounded with poor-Fe sphalerite (light gray), the next zone is chalcopyrite (gray) grading indistinctly to more ferrous sphalerite varieties (light gray) (Sample 3982-M1-2/1); e – reticulate exsolution texture of Cu, Fe, S solid solution: intergrowth of isocubanite (gray) and chalcopyrite (white) (Sample 3982-M1-6); f – pyrite streaks (dark gray) in Zn, Fe, S (light gray) and Cu, Fe, S (gray) matrix (Sample 3982-M1-3a); g, h – chalcopyrite segregation masses (white) in isocubanite (gray) (Sample 3982-M1-2/5a).

Table 7. Analyses of sphalerites and Cu,Fe-sulfides from the sulfide ores of the Rainbow hydrothermal field

Sample	Cu	Fe	Zn	S	Ag	Co	Cd	Au	$\sum$	Formula
						Sphalerite				
M1-2/3	0.93	22.98	39.03	34.77	0.00	1.57	0.20	n.d.	99.47	$Cu_{0.013}Fe_{0.379}Zn_{0.55}Co_{0.025}Cd_{0.002}S_{1.000}$
M1-2/1	0.80	23.95	39.55	34.15	0.04	1.25	0.00	n.d.	99.75	$Cu_{0.012}Fe_{0.403}Zn_{0.568}Co_{0.02}S_{1.000}$
M1-2/5a	5.00	15.17	44.79	33.53	0.00	0.38	0.17	n.d.	99.04	$Cu_{0.075}Fe_{0.260}Zn_{0.655}Co_{0.006}Cd_{0.001}S_{1.000}$
M1-6	0.65	17.99	46.61	34.14	0.05	0.87	0.18	n.d.	100.50	$Cu_{0.010}Fe_{0.302}Zn_{0.669}Co_{0.014}Cd_{0.002}S_{1.000}$
M2-2/2	0.78	14.69	49.24	34.40	0.04	0.42	0.05	n.d.	99.62	$Cu_{0.011}Fe_{0.245}Zn_{0.702}Co_{0.007}S_{1.000}$
M2-2	0.73	9.69	54.06	32.98	0.13	0.01	0.61	n.d.	98.21	$Cu_{0.011}Fe_{0.169}Zn_{0.804}Ag_{0.001}Cd_{0.005}S_{1.000}$
M1-3	0.35	10.05	56.73	34.59	0.00	0.14	0.09	n.d.	101.94	$Cu_{0.005}Fe_{0.167}Zn_{0.804}Co_{0.002}Cd_{0.001}S_{1.000}$
M1-2/5a	0.38	1.77	65.89	33.48	0.02	0.09	0.00	n.d.	101.65	$Cu_{0.006}Fe_{0.030}Zn_{0.965}Co_{0.002}S_{1.000}$
						Cu,Fe sulfides				
M2-2	34.25	29.59	0.45	35.84	0.08	0.17	0.01	0.00	100.39	$Cu_{0.965}Fe_{0.948}Zn_{0.012}Ag_{0.001}Co_{0.005}S_2$
M1-4	34.51	29.83	0.02	35.29	0.00	0.14	0.00	0.00	99.80	$Cu_{0.987}Fe_{0.971}Zn_{0.001}Co_{0.004}S_{2.000}$
M1-2/3	31.29	32.22	0.57	36.04	0.05	0.37	0.00	0.00	100.54	$Cu_{0.876}Fe_{1.027}Zn_{0.016}Ag_{0.001}Co_{0.011}S_{2.000}$
M1-6	30.49	31.82	1.46	33.21	0.06	0.92	0.00	0.12	98.08	$Cu_{1.390}Fe_{1.650}Zn_{0.065}Ag_{0.002}Co_{0.045}Au_{0.002}S_{3.000}$
M1-2/5a	23.50	38.90	1.45	35.85	0.08	0.57	0.00	0.30	100.65	$Cu_{0.992}Fe_{1.869}Zn_{0.060}Ag_{0.002}Co_{0.026}Au_{0.004}S_{3.000}$
M1-2/1	23.27	39.15	0.81	35.39	0.06	0.80	0.00	0.19	99.67	$Cu_{0.995}Fe_{1.906}Zn_{0.034}Ag_{0.002}Co_{0.037}Au_{0.003}S_{3.000}$
M1-3	19.78	42.50	0.15	35.25	0.07	0.51	0.00	0.21	98.47	$Cu_{0.850}Fe_{2.077}Zn_{0.006}Ag_{0.002}Co_{0.024}Au_{0.003}S_{3.000}$
M1-2/5	19.25	43.59	0.14	35.80	0.08	0.74	0.00	0.13	99.74	$Cu_{0.814}Fe_{2.097}Zn_{0.006}Ag_{0.002}Co_{0.034}Au_{0.002}S_{3.000}$

n.d. – not determined.

perimental error (0.05 wt.%). None of the sphalerite grains analyzed (N=21) contained Pt traces, that is the main Pt concentrators were Cu,Fe-sulfides and possibly pyrite.

Therefore the percentage of Pt-bearing grains increases in the sphaleriteisocubanite (solid solution)–chalcopyrite–(pyrite) series. The position of pyrite in this series need be verified.

Co–Ni sulfides. The ores of the Rainbow field are characterized by very high Co contents. Our earliest studies of the Rainbow ores revealed that the highest Co contents (>1%) were restricted to the sphalerite–Cu,Fe-sulfide association in the central portions of the lipes [*Lein and Sagalevich,* 2000]. The content of Ni in this sulfide association was found to be below analytical error (<0.02 wt.%). Minute grains of complex Ni–Co minerals were found in complex Ni–Co minerals in millerite and pentlandite at a contact between the chal-

copyrite and bornite zones [*Vikentiev et al.,* 2000]. These authors found millerite which, according to the results of an X-ray spectral analysis, contained Co (0.3–5.5 wt.%) and Fe (0.4–3.4 wt.%) in addition to Ni (41.0–47.5 wt.%). Pentlandite showed a lower Ni content (18.3–29.3 wt.%), often almost rqual to the contents of Co (9–23 wt.%) and Fe (9.7–12.9 wt.%).

The sphalerites of our collection showed a rather distinct positive correlation between the iron and cobalt contents. As the Fe content of sphalerite increases, their cobalt concentration declines (Figure 11, Table 7). The content of Co in Cu,Fe-sulfides is lower than in low-Fe sphalerite (Table 7). It appears that Fe and Co had been added to the hydrothermal solution from the same source. Because the clarke of Co concentration in the Earth's crust is significantly lower than the Ni concentration (the Co/Ni ratio varying from 0.31 to

Table 8. Compositions of pyrites and pyrrhotite from thesulfide ores of the Rainbow hydrothermal field (from microprobe analyses, wt.%)

Sample	Fe	Cu	Zn	Ag	Co	Cd	Au	S	$\sum$	Formula
M1-3a	46.80	0.01	0.16	0.05	0.03	0.00	0.00	52.79	99.85	$Fe_{1.018}Zn_{0.003}Ag_{0.001}Co_{0.001}S_{2.000}$
M1-3a	47.49	0.09	0.27	0.05	0.00	0.00	0.00	51.75	99.65	$Fe_{1.054}Cu_{0.002}Zn_{0.005}Ag_{0.001}S_{2.000}$
M1-3a	46.53	0.01	0.15	0.06	0.05	0.00	0.04	52.14	98.98	$Fe_{1.025}Zn_{0.003}Ag_{0.001}Co_{0.001}S_{2.000}$
M1-4a	46.79	0.34	0.18	0.00	0.00	0.00	0.19	52.81	100.31	$Fe_{1.018}Cu_{0.006}Zn_{0.003}Au_{0.001}S_{2.000}$
M1-4a	45.87	0.33	0.19	0.03	0.02	0.00	0.00	53.55	99.99	$Fe_{0.984}Cu_{0.006}Zn_{0.003}S_{2.000}$
M1-4a	45.29	0.07	0.26	0.00	0.04	0.00	0.00	53.44	99.10	$Fe_{0.973}Cu_{0.001}Zn_{0.005}Co_{0.001}S_{2.000}$
M1-4a*	58.85	0.02	0.24	0.05	0.14	0.00	0.00	38.84	98.15	$Fe_{0.870}Zn_{0.003}Co_{0.002}S_{1.000}$
M1-4a	45.53	0.00	0.08	0.01	0.17	0.00	0.01	52.80	0.00	$Fe_{0.990}Zn_{0.002}Co_{0.003}S_{2.000}$

* denotes pyrrhotite analysis.

Table 9. Analyses of native accessory minerals from the Rainbow field, wt.%

Sample	Fe	Cu	Au	Ag	Zn	Cd	$\sum$	Ore type
4b(1)	–	–	95.7	4.3	–	–	100.0	Cu
4b(2)	–	–	95.6	4.4	–	–	100.0	Cu
3a	0.5	0.4	–	–	–	99.0	99.9	Cu
2/7	1.8	–	–	–	4.7	93.6	100.1	Zn

4b(1)–gold $(Au_{0.94}Ag_{0.06})_{1.00}$
4b(2)–gold $(Au_{0.94}Ag_{0.06})_{1.00}$
3a–native cadmium $(Cd_{0.98}Cu_{0.01}Fe_{0.01})_{1.00}$
2/7–native cadmium $(Cd_{0.98}Fe_{0.01}Cu_{0.01})_{1.00}$.

0.34 according to different investigators), one could expect a relatively high Ni content in sulfides. However a detailed study of the sphalerite chemistry did not confirm this expectation. This means that Ni and Co differentiation had taken place prior to the formation of the hydrothermal solution. The cause of this differentiation might have been a difference in the behavior of Ni^{2+} and Co^{3+} ions. In any case the enrichment of sulfide associations in Co (a positive, though less distinct correlation between Fe and Co is traceable not only in sphalerite but also in Cu,Fe-sulfides) is a proved fact, and the high Co/Ni ratio in sulfides can be another proof for establishing a genetic relationship between submarine hydrothermal ore deposition and massive sulfide deposits, for which Co/Ni$\geq$1 [*Ivanov,* 1996].

The most widespread nonmetallic mineral is anhydrite. Sometimes the outer hydroxide crusts are made of barite or opal (Figure 14). Opal may also cement the fragments of the sulfide pipes producing specific breccia-like structures. Anhydrite is mainly found in sphalerite and chalcopyrite sphalerite ores and can form pipes of anhidrite composition, in which growths with fine-grained sulfide minerals can be found.
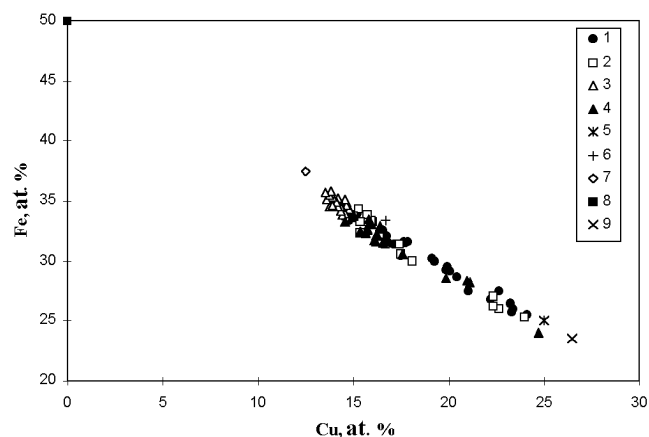
Figure 12. Variations of Cu,Fe sulfide composition from the center of the structure (Sample 3982-M1-2): 1 – top of the sample, 2 – middle, 3–4 – base; 5 – $CuFeS_2$, 6 – $CuFe_2S_3$, 7 – $CuFe_3S_4$, 8 – FeS, 9 – talnakhite.
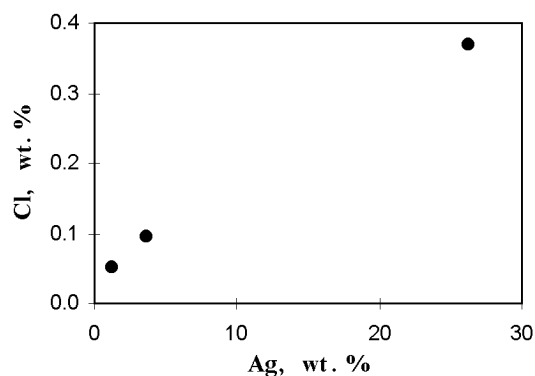
Figure 13. Positive correlation of Ag and Cl concentrations in silver-rich sulfide phases (Sample 3982-M1-2).

Table 10. Platinum content of sulfide minerals from submarine hydrothermal structures in the Rainbow field

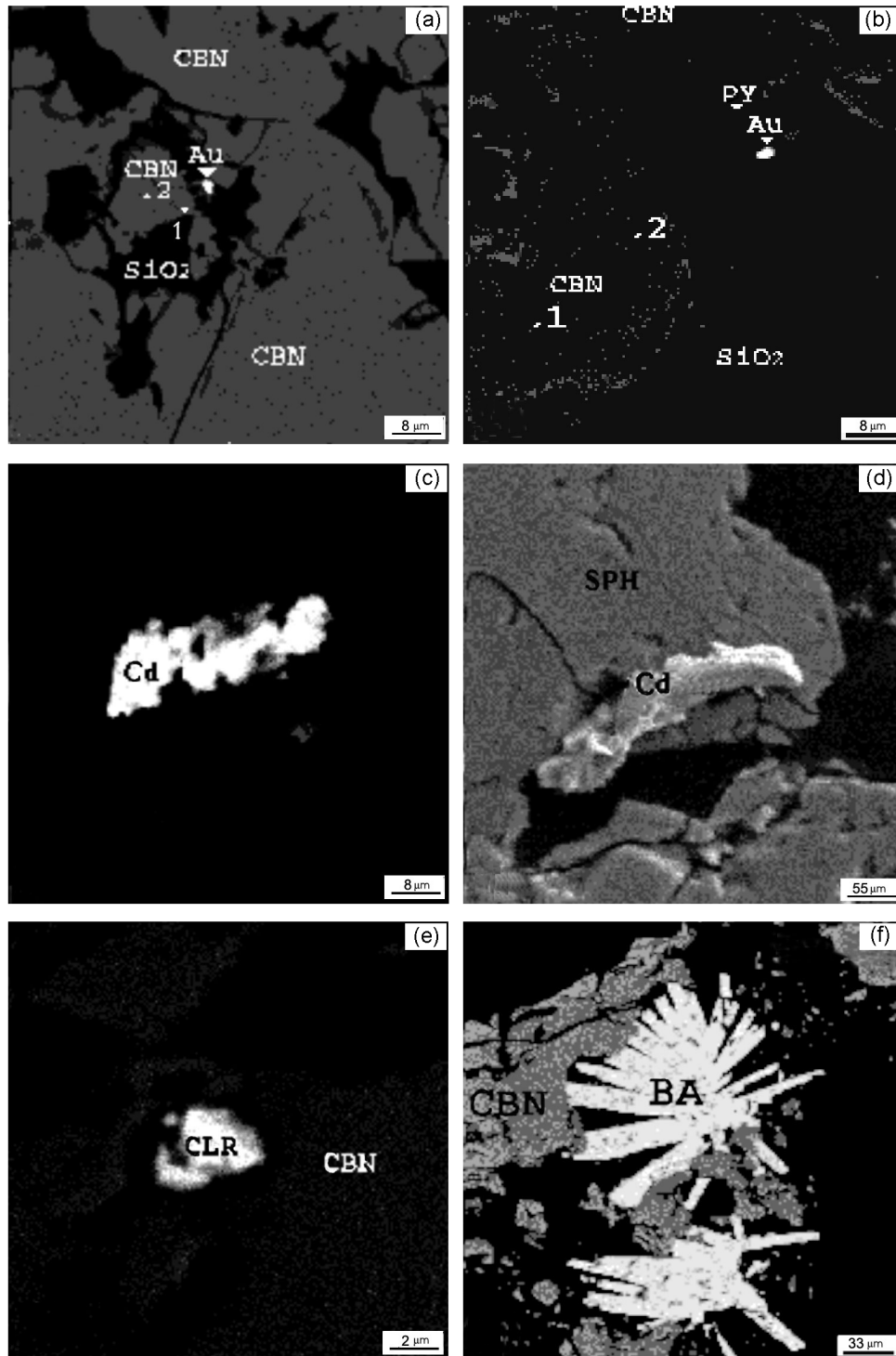| Sample	Mineral	Total number of analyzed grains	Number of grains with Pt>0.05 %	% Pt-bearing grains	Pt, wt.%
M1-4a	chalcopyrite	8	3	37.5	0.10–0.23
M1-2/1 M1-2/5a M1-3a	cubanite-based solid solution	20	4	20	0.05–0.34
M1-3a	pyrite	2	1	50	to 0.14
M1-2/1 M1-2/3 M1-2/5b M1-3a M1-4a M1-6 M2-2 M2-2/2	sphalerite	21	0	0	<0.05

Figure 14. Accessory minerals in the ores of the Rainbow field (Site 3982-M1): a – native gold (Au) in opal (SiO_2) filling interstices in isocubanite (CBN); b – native gold at contact with isocubanite (Sample 4b: points 1 and 2 correspond with the respective analyses in Table 9); c – cadmium grains (Cd, Sample 3a); d – cadmium grains in sphalerite (Sample 2/7); e – coloradoite (CLR) in cubanite (Sample 3a); f – barite (Ba) stars in isocubanite (Sample 3). Photographs a, b, c, e, and f are in reflected electrons, d – in secondary electrons.
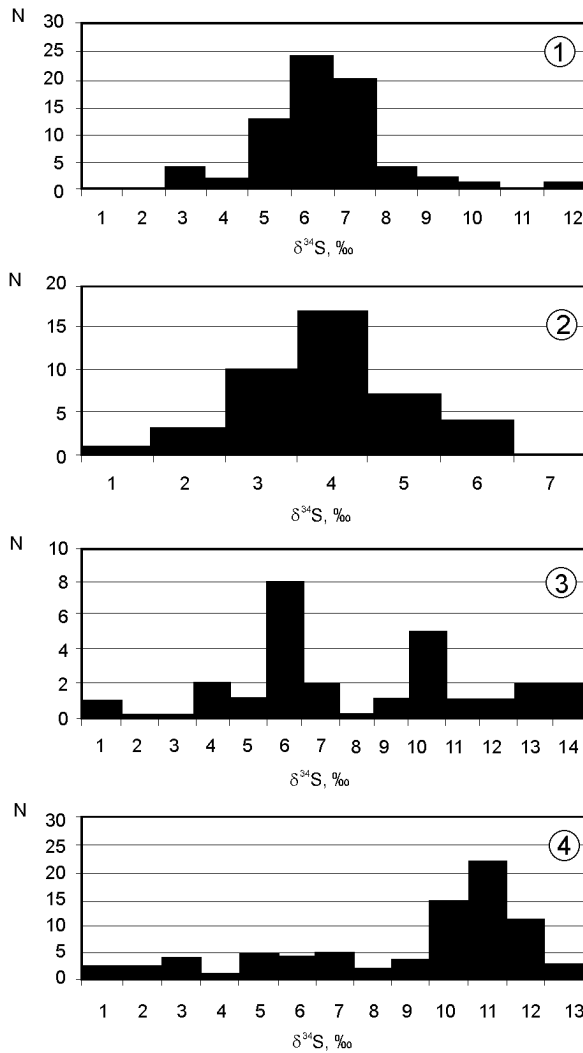
Figure 15. A histogram of $\delta^{34}S$ values for the MAR hydrothermal fields: 1 – TAG, 2 – Broken Spur, 3 – Logachev, 4 – Rainbow.

Table 11. Isotopic composition of sulfide sulfur from the Rainbow field

Sample no.	$\delta^{34}S,^o/_{oo}(CD)$		
	Sphalerite	Cu,Fe-sulfides	Pyrite
St. 3840-M1			
2-5	9.9	9.2	
2-6	8.3	9.0	
3-1a	10.4	9.3	
3-1b	8.4	10.0	
4-4a	10.3	10.2	
4-4b	9.1	10.3	
5-3a	10.3	9.6	
5-3b	8.6	10.2	
5-3c	8.6	11.1	
10-1	9.9	10.2	
11-3	9.9	10.7	
12-1a	9.3	12.1	
12-1b	11.4	11.5	
12-3a	9.9	10.8	
12-3b	10.4	11.0	
13-2a	10.1	11.2	
13-2b	10.7	12.5	
13-4	9.8	10.6	
St. 3982-M1			
1			0.5
2-2	9.7	10.0	
2-3	6.7	9.3	
2-5	9.4	9.7	
3		10.3	
4-a1		6.1	
4-a2		5.2	
4-b		5.9	
5	5.3	7.0	
	5,9	7.6	
St. 3959-M1			
3 (core)	1.3	2.0	
(margin)	2.6	2.9	

According to the results of the thermobarometry and geochemistry of primary inclusions in anhydrite from the ores, the temperature of anhydrite formation was 177°–198°C [*Simonov et al., 2000*]. In the almost monomineral anhydryte portions of the pipes the temperature of anhydrite formation (based on primary inclusions) was as high as 316°–370°C [*Simonov et al., 2000*]. Judging by the character of relationships between anhydrite and sulfide minerals, Ca sulfate can precipitate from solutions of different temperatures simultaneously with sulfide minerals: sphalerite and Cu,Fe-sulfides.

As regards accessory minerals, worthy of mention is a Cd-rich mineral (supposedly native Cd) found in Samples 3982-M1-3a and 3982-M1-2/7 in association with Cu-minerals and sphalerite, respectively (Table 9, Figure 14c and d). Its calculated formula is $(Cd_{0.98}Cu_{0.01}Fe_{0.01})_{1.00}$.

Sulfur Isotope Composition in the Ores of the Rainbow Field

The sulfur isotope composition of the sulfides was studied using the fragments of relict sulfide pipes and one active black smoker found on the slopes of the old and relatively young Rainbow structures, respectively (Figure 15, Table 11).

More comprehensive isotope determinations were obtained for the sulfide sulfur from the active structures in the central part of the Rainbow field. The $\delta^{34}S$ values of the sulfide ores from the relict pipes range between 5.2 and 12.5$^o/_{oo}$ with the mean value of 9.8$^o/_{oo}$ for sphalerite and 10.6$^o/_{oo}$ for Cu,Fe-sulfides and Fe-sulfides (Table 11).

Table 12. Summary table of Rainbow sulfyr isotope composition

Mineral	Number of samples	Variation range δ^{34}S, $^o/_{oo}$(CD)	Av. δ^{34}S,$^o/_{oo}$
Inactive smokers of unknown age			
chalcopyrite (bornite + pyrite?)	31	9.0–12.5	10.6
sphalerite	20	8.3–11.4	8.8
Old inactive smokers, age $\sim$2.0–2.3 thou. years			
chalcopyrite (bornite + pyrite?)	5	9.3–10.3	9.8
sphalerite	3	6.7–9.7	8.6
Young inactive smokers, age 2.2–3.1 thou. years			
chalcopyrite (bornite + pyrite?)	5	5.2–7.6	6.4
sphalerite	2	5.3–5.9	5.6
Modern active (smoking) smoker			
chalcopyrite	2	2.0–2.9	2.5
sphalerite	2	1.3–2.6	1.9
anhydrite	2	19.8–20.3	20.0
Black-smoke sulfide suspension			
pyrrhotite + CuFeZn-sulfide	3	2.4–3.3	2.8
Hydrogen sulfide of hydrothermal solution with t = 362°C			
HS$^-$-ion (as Cd acetate)	2	2.4–3.1	2.7
Serpentinite			
sulfide veinlet	1	0.5	0.5

Total 78 samples.

It should be noted that in the paragenetic sulfide assemblages the δ^{34}S values for sphalerite were found to be isotopically lighter than the sulfur of the Cu,Fe-sulfides or identical (Tables 11, 12).

No changes were found in the isotopic composition of sulfur from the sulfides in the vertical sections of the pipes. For instance, the ore samples collected at Site 3982-M1-2 from the base (a), middle (b), and top (c) of the pipe showed almost invariable δ^{34}S values for the sulfide minerals from the ore matrix (Table 11).

An indistinct zonal pattern in the distribution of δ^{34}S values for sulfides was found occasionally in the horizontal saw cuts of the pipes in the direction from a gently dipping or healed central conduit to the outer zone of the pipe. In these cases the pipe cuts showed the recrystallization and the heavier sulfur of sphalerite and Cu,Fe minerals in the outer zone compared to the loose sooty matrix in the central part of the pipe (Table 10).

The isotopic composition of sulfur was not determined in the ores of the Logachev-2 field.

Lead Isotope Composition of Rocks and Ores in the Logachev-1 and Rainbow Fields

Lead isotopes are known to be more effective tracers of the sources of metals. The presence of lead in the sulfide ores of recent hydrothermal fields allowed to use its isotope composition to establish the source of the metallic matter [*Andrieu et al.,* 1998; *Bibikova et al.,* 1993; *Cherkashev et al.,* 2001; *Dupre et al.,* 1988; *Grichuk and Lein,* 1991; *Hamelin et al.,* 1984; *Hegner and Tatsumoto,* 1987; *Lein et al.,* 1988, 1991]. These authors reported the results of studying lead isotope compositions of ores mainly from the axial parts of the hydrothermal systems associated with basalt volcanism. In this paper we describe the results of studying lead isotopes in rgw sulfide ores of the Rainbow and Ligachev-1 fields, produced by the deep circulation of the system (Table 12). The Pb contents in the Rainbow ores averaged 0.036% (Table 2). The highest lead concentrations (max. 0.2752 at Site 3840-1-2) were found in the goethite–hematite–magnetite–sulfide

mineral asssociation in the sulfide–Fe oxide crust of the pipe. The Pb concentrations varied from 100 to 785 ppm in the primarily Zn sulfide ores, the lowest (<5 ppm) Pb contents were found in the Cu- and Fe-sulfides. The electron microprobe measurements of the rainbow sulfides revealed galena as an independent mineral phase (Table 5). The galena was found to contain 1.87 to 12.84% Zn (mechanical admixture of sphalerite), 3.26 to 6.33% Se, and less than 1% Fe. The resulting isotope characteristics of lead from the sulfides and serpentinite of the two studied fields are compared in Figure 16 with the curves of the lead evolution in the mantle, upper and lower crust, and the "orogenic belt", calculated using the plumbotectonic model proposed in [*Doe and Zartman,* 1979]. It is known that the lead isotope compositions of the sulfides associated with MORB basalts in axial hydrothermal circulation systems reside near the mantle curve of lead evolution within a 18.0–18.4 range. The lead isotope values of the Rainbow (18.5–18.8) and Logachev (18.9–19.3) fields are highly displaced to the left from the values characteristic of all other sulfides known from oceanic ore occurrences. In terms of the $^{207}Pb/^{204}Pb$ ratio the leads of these fields fall into the range of the values typical of the leads from the lower crust and mantle and are notably displaced toward radiogenic sulfides. In other words, the main sources of metals (lead) in the ores of the Logachev-1 and Rainbow fields were the rocks of the lower crust and mantle.

Discussion of Results

The results of previous investigations proved that like the Logachev-1 field the Logachev-2 and Rainbow hydrothermal fields were restricted to serpentinite protrusions "squeezed" out to the ocean floor surface along the raised block of a marginal tectonic scarp (Logachev-1 field) and along the axial fissure of the spreading origin (Rainbow field) [*Bogdanov et al.,* 1997, 1999; *Cherkashev et al.,* 2000]. It is believed that the deep hydrothermal circulation system, acting on these two fields, was controlled by tectonic processes and activized by the exothermal processes of serpentinization. An important specific feature of the primary hydrothermal solutions (PHS) of both fields are long-lasting intermittent temperature variations, sometimes as high as a few tens of degrees (240–308°C) and the high content of chlorine in the studied samples of a hot fluid, 1.4 times higher than its content in oceanic water [*Bogdanov et al.,* 1997, 1999; *Lein et al.,* 2000].

These two parameters of the solutions suggest a constant inflow of cold sea water into the subsurface portions of the hydrothermal system. An example is a temperature difference of solutions during the precipitation of anhydrite, a ubiquitous mineral in the Logachev and Rainbow hydrothermal structures. This temperature difference was recorded during the study of gas–liquid inclusions in this mineral. The temperatures of anhydrate formation were found to vary from 177–198°C to 316–370°C [*Simonov et al.,* 2000].

The high concentration of a Cl⁻-ion in the solution leads to its abnormally high enrichment in metals. For instance, the iron concentration in the primary hydrothermal solution
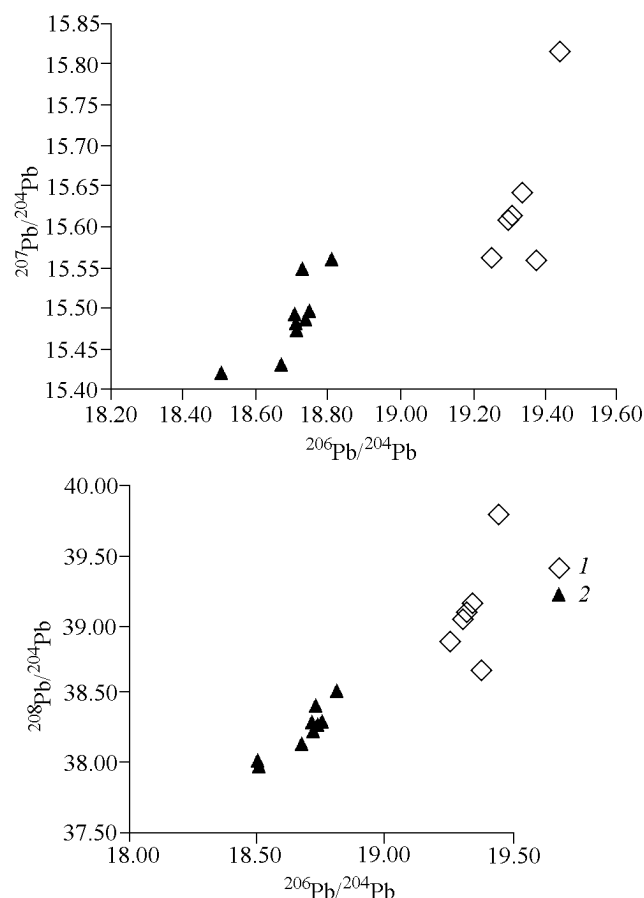

Figure 16. Lead isotope composition in the sulfides of the Logachev (1) and Rainbow (2) fields.

(PHS) of Rainbow is 5 to 12 times higher than in the solutions of the Logachev-1, TAG, Broken Spur, and Snake Pit fields, and more than 24 higher than in the solutions of the Lucky Strike and Menez Gwen shallow-sea fields (Table 13). The Rainbow solutions are enriched in Cd, Zn, Ag, Mn, and especially Co (Table 13). The sources of metals are ultramafic rocks, as confirmed by the lead isotope ratios in the ores (Figure 16). The abnormally high H_2 and CH_4 concentrations with low H_2S contents is another typical feature of the primary hydrothermal solutions of the Logachev-1 and Rainbow fields, a feature also related to the ultramafic composition of the source rocks involved in the deep hydrothermal circulation system [*Bogdanov et al.,* 1997, 1999; *Lein et al.,* 2000]. It is possible that part of its hydrogen sulfide is oxidized by oxygen from the cold oceanic water involved into the hydrothermal system.

The low H_2O concentratiom in the solutions of the Rainbow field might have been responsible for the abnormally high Fe content in it (Table 14), and also for the precipitation of iron oxides: magnetite and hematite (Table 14), limonite, goethite, and hydrogoethite.

The sulfur in the H_2S fluid and in sulfide minerals from the suspensions in the Rainbow and Logachev-1 fields contains less ^{34}S isotope compared to the sulfur of the sulfides

Table 13. Chemical composition of primary hydrothermal solutions from MAR active fields, modified after [*Desbruyeres et al.,* 2001]

	Hydrothermal field	Menez Gwen	Lucky Strike	Rainbow	Broken Spur	TAG	Snake Pit	Logachev
C°	T	263–284	152–333	360–365	356–364	270–363	335–356	>353
	pH	4.2–4.8	3.5–4.9	2.8–3.1		2.5–3.4	3.7–3.9	<3.3
mm/kg	Si	8.2–11.2	9.1–17.5	6.9–8.0		18–22	18–20	7–8.2
	Cl^-	360–400	410–540	>750	469	633–675	550–563	515–522
	CO_2	17–20	8.9–28	<16		2.9–4.1	10.63	
	H_2S	1.5–2	1.4–3.3	1–2.5	9.3	2.5–6.7	2.7–6.1	<1
	CH_4	1.35–2.63	0.5–0.97	2.2–2.5	0.065	0.14–0.62	0.046–0.062	2.1
	Fe	0.002–0.018	0.13–0.86	24	1.68–2.16	1.64–5.45	1.8–2.56	2.50
	Mn	0.068	0.45	2.25	0.26	1	0.49	0.33
μm/kg	Cu*			30	68.6	120–150	12	
	Zn*			160	88	46	47	
nm/kg	Co*			7500	422			
	Cd*			2000–2300	145			
	Pb*			230–250	376			
	Ni*			130–190				
	V*			150				
	Ag*			120				
	Au*			13				

* after [*Lein et al.,* 2000]

from the main paragenetic ore association (Tables 11, 12, 14). The isotopically lighter composition of sulfur from the H_2S hydrothermal fluids compared with the S isotope composition of the sulfide ores is not a new fact. It was recorded in the ore fields of the 11–13°N East Pacific Rise, the Axial Mount on the Juan de Fuca Ridge, and TAG [*Gamo et al.,* 1997; *Grichuk,* 2000; *Hannington and Scott,* 1988; *Lein et al.,* 1993].

Therefore the chemical composition of the primary hydrothermal solution of the Rainbow field was controlled, like that of the Logachev-1 field, by the following thre main processes; (1) the interaction between water and ultramafic

Table 14. Concentration and isotopic composition of gases from MAR hydrothermal fluids [*Lein et al.,* 2000]

Dissolved gases		Oceanic water	Hot fluides of hydrothermal fields					
			Rainbow*	Logachev*	TAG	Broken Spur	Snake Pit	Lucky Strike
H_2S		0.000	2.0–2.5	2.5–3.0	3.5–6.7	8.5–11.0	6.0	2.5–3.0
NH_4	mm/kg	<0.01	<0.01	–	3.65	1.21	–	–
CO_2		2.3	2.9–3.1	2.8–3.0	2.9–3.4	6.0–7.1	–	13.0–28.0
H_2		0.0004	13.000	12.600	152–370	426–1026	22.0	20.0–726
CH_4	μm/kg	0.0004	2200	2310	124–147	65–130	45–100	500–970
N_2		590	–	–	800–890	–	–	–
δ^{34}S-H_2S(CD)		–	2.4–3.1	2.2–2.8	1.1–2.5	0.5–1.0	4.9–5.0	–
δ^{13}C-CH_4 $^o/_{oo}$(PDB)		–	$-13.0 \div -13.4$	$-13.8 \div -14.6$	-15.0	$-18.0 \div -19.0$	–	–
δ^{13}C-CO_2(PDB)		$1 \div -4$	$1 \div -4$	-4.3	-5.6	-9.0	–	–

* Gas contents of solutions were measured using a chromatograph with a flame-ionization detector (HPM–2). The isotopic compositions of dissolved gases (δ^{13}C-CH_4, δ^{13}C-CO_2 δ^{34}S-H_2S) were measured using a modified 2-beam mass-spectrometer MI–1201B ("Electron") after the transformation of gases to CO_2 and SO_2. Accuracy $\pm 0.2^o/_{oo}$.

rocks (serpentinite), operating at high temperature ($>362°$) and pressure; (2) a phase separation of the primary hydrothermal solution in the subsurface environment, which produces metal-rich chloride brines, and (3) the inflow of oceanic water into the subsurface interval of the hydrothermal systems, which lowers the temperature and salt composition of the solutions and oxidizes H_2S. In other words, the primary hydrothermal solution of the Rainbow field (and Logachev-2 field) is a mixture of brine, a vapour-gas phase, depleted H_2S, and altered sea water.

The experimental data obtained in this study of the chemical and mineral compositions of ores from the Logachev-2 and Rainbow fields prove their copper–zinc metallogeny, the fact distinguishing them from the ores of the Logachev-1 field with prominent copper metallogeny [Bogdanov et al., 1997]. Moreover the chemical compositions of the Rainbow and Logachev-2 ores have some features in commom, which distinguish them from all known MAR ore occurrences: they are 5 times higher in Zn, 20 times higher in Co, and 5 times higher in Ni (Table 2). The ores of the Logachev-2 field also have high Au concentrations, and the Rainbow ores have Ag concentrations which are 4 times higher than the average values for the MAR ores (Table 2).

Based on the results of our mineralogical studies, we dsitinguished the following three major phases of ore generation:

(1) the early high-T, predominantly pyrrhotite phase, its minerals being almost wholly replaced by Cu,Fe-sulfides and sphalerite;

(2) the main ore-formation phase with a paragenetic association consisting of sphalerite, containing different amounts of iron, and Cu,Fe-sulfide minerals, mainly isocubanite and chalcopyrite: Zn,Fe- and Cu,Fe-sulfides were deposited almost simultaneously from intermittently flowing, nonequilibrium and different-temperature solutions without reaching a solid phasefluid equilibrium;

(3) the late phase of mineral recrystallization and substitution and the filling of interstices and voids by minerals from new fluid portions.

Iron disulfides (pyrite and marcasite) are rare. Occasionally found were magnetite and some rare Cd, Te, and other minerals.

As regards nonmetallic minerals, anhydrite occurs ubiquitously in all ther paragenetic associations, and also silica minerals and barite.

The presence of hypogene iron minerals, goethite and hematite, was obviously caused by the low content of H_2S in the solution and by the addition to the system of a strong oxidizing agent – cold oceanic water.

We failed to find any regularities in the variations of the contents of secondary elements in the coexisting sphalerite and Cu,Fe-sulfides (Figure 12). The Co and Ag distribution, the absence of linear two-element functions, and the significant variations in the contents of secondary elements in the coexisting sphalerite and Cu,Fe-sulfides suggest that no equilibrium was attained during the formation of the metallic mineral association, and that the ore deposition was a rapid process, the fact confirmed by the absence of stoichiometry of the Cu,Fe-sulfides.

Our mineralogical studies of ores from the Rainbow and Logachev-2 fields confirmed confirmed the previously established [Lein et al., 2000] fact of the high variations of the chemical composition and temperature of the ore-forming fluid during the deposition of the paragenetic mineral assemblages at the main stage of ore deposition, the fact not so typical of the other ore fields in the ocean (except Logachev-1).

As regards the geochemistry of the ore deposition process in the Rainbow and Logachev-1 hydrothermal systems, of particular interest are the results of the isotopic analysis of sulfur from the sulfide ores. As follows from the data presented in Tables 11 and 12 and in Figure 15, the $\delta^{34}S$ values of sulfur for the sulfides from both fields are highly enriched in ^{34}S isotope, even compared with the sulfide minerals of the TAG mature system, let alone the young sulfide ores of the Broken Spur, which inherited their $\delta^{34}S$ values from the sulfur in the basalts.

The more isotopically heavy bornite mineral assemblage from yje outet zones of the sulfide pipes was formed undoubtedly with the paticipation of the sulfate ion of cold oceanic water. Along with the isotopically heavy sulfides of the main paragenetic assemblage, the Rainbow ores contain isotopicaly light sulfide minerals with $\delta^{34}S = 1.3$–$2.9°/_{oo}$, produced during the late phase of ore deposition (Tables 11 and 12). These minerals are usually found in ore cavities. In spite of their scarce development, these isotopically light varieties of sulfide minerals were described earlier from the Logachev-1 ores [Bogdanov et al., 1997]. These authors mentioned the "extreme heterogeneity of the sulfur isotope composition in sulfides". They explained this heterogeneity by the fractionation of sulfur isotopes in hydrogen sulfide during the phase separation of primary hydrothermal solutions. It should be noted that practically no fractionation of sulfur isotopes takes place during this phase separation. Therefore an almost $14°/_{oo}$ difference for sulfur from different sulfide minerals of the Logachev and Rainbow fields must have another explanation. Moreover, the ranking of sulfide minerals with different phases of the ore formation process masks the impression of the heterogeneity of their isotope composition. On the contrary, the $\delta^{34}S$ values in the minerals of the main paragenetic assemblage are very close and fit within a narrow range of 7 to $10°/_{oo}$ (Tables 11 and 12).

Therefore the sulfide minerals from the pipes of the Rainbow (and Logachev-1) field are more enriched in heavy ^{34}S isotope (Figure 15), compared with the other MAR fields, and are highly different isotopically from the hydrogen sulfide of the hot fluids. Explanation still need be found for the light isotope composition of sulfur in the H_2S of the primary hydrothermal solutions in the Rainbow and Logachev-2 fields with the heavy isotope composition of their sulfide ores.

A model of a multiwave, flow-through, multistep reactor was offered by Grinchuk [2000] for a long-lived hydrothermal system, which admits, in an isothermal section of about $370°C$, a change in the isotope composition of hydrogen sulfide in the solution from $10°/_{oo}$ to nearly zero at the instant of the inflow of oxidizing sulfate solutions. Consequently, the model does not prohibit the possibility of hydrogen sulfide losing its heavy isotope in a system where oceanic water is added.

Table 15. Isotopic composition of lead from serpentinite (Sample 3982-M1-1) and Cu-sphalerite ore (Sample 3982-M1-2-6) from the Rainbow field

Sample no.	$^{206}Pb/^{202}Pb$	$^{207}Pb/^{204}Pb$	$^{208}Pb/^{204}Pb$
M1-1	18.508	15.547	38.007
M1-2/1	18.808	15.560	38.511
M1-2/3	18.717	15.474	38.230
M1-2/5	18.767	15.518	38.386
M1-2/5a	18.740	15.489	38.274
M1-2/7	18.715	15.492	38.294
M1-3	18.509	15.422	37.981
M1-3a	18.676	15.434	38.130
M1-4b	18.729	15.549	38.412
M1-4c	18.751	15.499	38.303
M1-5	18.733	15.487	38.290
M1-6	18.717	15.480	38.232

Analyst B. V. Belyatskii, Institute of Precambrian Geology and Geochronology, Russian Academy of Sciences.

Another possible mechanism is that the poorly oxidizing properties of the solution, from which hypogene iron oxides precipitate, permit some half-oxidized sufur compounds (hydrogen polysulfide, polythionate, etc.) to be present in the solution. These hypothetic semioxydized sulfur compounds were not looked for and, hence, not analyzed, even though they might have participated, along with the H_2S of the solution, in the formation of isotopicaly heavy sulfide minerals in the Rainbow and Logachev fields. It is impossible to verify the presence of such sulfur compounds in the solution using the models available, because the calculation of the composition of the primary hydrothermal solution assumes a priori the absence of oxydized sulfur compounds in it. A difference between the isotopic composition of sulfur in the hydrogen sulfide of the primary hydrothermal solution and in the sulfide ores of the Rainbow and Logachev-1 fields remains to be an enigmatic phenomenon which requires a special study of all sulfur compounds in the hot fluids of the Rainbow and Logachev-1 fields.

Conclusions

1. The sulfide ores of the Logachev-2 and Rainbow fields are restricted to serpentinite protrusions and have a copper–zinc metallogeny in contrst to the ores of the Logachev-1 field with its distinct copper metallogeny. Consequently, the initial rocks (ultramafics, serpentinite, and others) did not controlled the metallogeny of the ores associated with them.

2. The Zn(Fe) and Cu–Fe(Zn) sulfides precipitated in the pipes of black smokers almost simultaneously with from intermittently flowing nonequilibrium H_2S solutions.

3. Like the ores of the Logachev-1 field, the sulfide minerals of the Rainbow field are enriched in heavy ^{34}S isotope ($\delta^{34}S_{av} = 10^o/_{oo}$), which was possibly associated with the participation in their formation (along with isotopically light H_2S) of semioxidized, isotopically heavy sulfur compounds, the potential source of which might have been cold oceanic water which flowed perpetually into the subbottom zones of the hydrothermal system.

4. The isotope conposition of lead from the ores of the Rainbow field is comparable with that of the host serpentinites and differs from the lead isotope composition of all MOR fields restricted to oceanic basalts, occupying a position intermediate between the ores of these fields and those of the Logachev-1 field (Table 15). The values of the lead isotope ratios for the Rainbow and Logachev fields lie on the curve characteristic of the rocks of the lower oceanic crust (ultramafics and serpentinite), thus indicating the source of metals from the deep layers of the oceanic crust.

5. The ores of the Logachev-2 and Rainbow fields are 5 times higher in zinc and 4 times higher in cadmium than the ores of the other MAR fields.

6. The ores of the Rainbow field contain 20 times more Co than the ores restricted to basalts and 8–10 times more Co than the ores of the Logachev-1 and -2 fields associated with serpentinites. The Rainbow ores are marked by the highest Co/Ni value equal to 46.

7. The chemical analyses of the bulk samples showed that the ores of the Rainbow field were 5 times higher in silver, and those of the Logachev-2 field were 8 times higher in gold than the other MAR ore fields. Native gold grains were found mainly in silica minerals filling voids in the soft porous portions of the sulfide pipes.

8. The sulfide ores of the Rainbow and Logachev-2 fields have no analogs among the MAR ore occurences in the contents of useful components (Zn, Cd, Co, and Au).

References

Andrieu, A. S., J. Y. Honnorez, and J. Lancelot, Lead isotope composition of the TAG mineralization, Mir-Atlantic Ridge, 26°08′ N, *Proc. Ocean Drilling Program. Scientific Results, 158,* (8), Eds. P. M. Herzig et al., 101–109, 1998.

Barriga, F. F. A., I. M. A. Costa, J. M. R. Relvas, et al., The Rainbow serpentinites and a serpentinitesulfide stockwork (Mid-Atlantic Ridge, AMAR segment): A preliminary report of the Flores results, *EOS. Amer. Geophys. Union. Translation, 78,* (46), F832, 1997.

Bibikova, E. V., T. V. Gracheva, A. Yu. Lein, et al., The source of metals for present-day ocean-floor ore deposition from the analysis of lead isotope data, in *Isotopic Dating of Endogenic Ores,* pp. 84–91, Nauka, Moscow, 1993.

Bogdanov, Yu. A., A. N. Sagalevich, E. S. Chernyaev, et al., Hydrothermal field at $14°45'$ N Mid-Atlantic Ridge, *Doklady Ross. Akad. Nauk, 365,* (5), 1995.

Bogdanov, Yu. A., N. S. Bortnikov, I. V. Vikentiev, et al., A new type of a present-day mineral deposition system: Black smokers of a hydrothermal field at $14°45'$ N Mid-Atlantic Ridge, *Geol. Rudn. Mestorozhd., 39,* (1), 68–90, 1997.

Bogdanov, Yu. A., A. M. Sagalevich, E. G. Gurvich, et al., Submarine geological survey of the Rainbow hydrothermal field (Mid-Atlantic Ridge), *Doklady Ross. Akad. Nauk, 365,* (5), 657–662, 1999.

Bogdanov, Yu. A., N. S. Bortnikov, E. G. Gurvich, et al., Hydrothermal fields on the serpentinite massifs of the Mid-Atlantic Ridge, in *Metallogeny of Old and Present-Day Oceans–2000,* pp. 49–53, Ural Division, Russian Academy of Sciences, Mias, 2000.

Borodaev, Yu. S., N. N. Mozgova, T. V. Stepanova, and G. A. Cherkashev, Precious metals in the sulfides of the Logachev hydrothermal field (Mid-Arlantic Ridge, $14°45'$ N), *Vestn. Mosk. Univ., Ser. 4. Geologiya,* (3), 40–49, 2000.

Grichuk, D. V., *Thermodynamic Models of Submarine Hydrothermal Fields,* 303 pp., Nauchnyi Mir, Moscow, 2000.

Grichuk, D. V., and A. Yu. Lein, Evolution of an oceanic hydrothermal system and the sulfur isotope composition of sulfides, *Doklady Ross. Akad. Nauk, 318,* (2), 422–425, 1991.

Cherkashev, G. A., B. V. Belyatskii, A. Yu. Lein, et al., Lead isotope ratios in the ore structures of the Mid-Atlantic Ridge, in *Proc. Conf. Geology and Geophysics of Mid-Oceanic Ridges,* 67, VNIIOkeangeologiya, St. Petersburg, 2001.

Cherkashev, G. A., A. M. Ashadze, and A. V. Gebruk, New fields with manifestations of hydrothermal activity in the Logachev area ($14°$ N, Mid-Atlantic Ridge), *InterRidge News, 9,* (2), 26–27, 2000.

Desbruyeres, D., A. Almeida, M. Biscoito, et al., A review of the distribution of the distribution of hydrothermal vent communities along the Northern Mid-Atlantic Ridge: Dispersal vs. environmental controls, *Hydrobiologia,* (1), 1–16, 2000.

Desbruyeres, D., M. Biscoito, Y. C. Caprais, et al., Variations in deep-sea hydrothermal vent communities on the Mid-Atlantic Ridge near the Azores Plateau, *Deep-Sea Research, Part 1, 48,* 1325–1346, 2001.

Doe, B. R., and R. E. Zartman, Plumbotectonics, The Phanerozoic, *Geochemistry of Hydrothermal Ore Deposits, Chapter 2,* 22–70, Wiley Intern. Publ., N.Y., 1979.

Dupre, B., G. Blank, Y. Bonlevgue, and C. J. Allevgre, Metal remobilization at spreading centers, using lead isotopes, *Nature, 333,* 165–167, 1988.

Fouquet, Y., J. -L. Charlou, H. Ondreas, et al., Discovery and first submersible investigations on the Rainbow hydrothermal field on the MAR ($36°14'$ N), *EOS. Amer. Geophys. Union Translation, 78,* (46), F832, 1997.

Gamo, T., K. Okahura, J. L. Charlou, et al., Acidic and Sulfate-rich hydrothermal fluids from the Manus back-arc basin, Papua New Guinea, *Geology, 25,* (2), 139–142, 1997.

Hamelin, B., B. Dupre, and C. J. Allevre, Pb–Sr variations along the Pacific Rise and Mid-Atlantic Ridge: A comparative study, *Earth Planet. Sci. Lett., 67,* 340–350, 1984.

Hannington, M. D., and S. D. Scott, Mineralogy and geochemistry of a hydrothermal silica–sulfide–sulfate spire in the caldera of an axial seamount, Juan de Fuca Ridge, *Can. Mines., 26,* (3), 603–625, 1988.

Hegner, E., and M. Tatsumoto, Pb, Sr, and Nd in basalts and sulfides from Juan de Fuca Ridge, *J. Geophys. Res., 92,* 11,380–11,386, 1987.

Ivanov, V. V., *Ecological geochemistry of elements,* Book 4, pp. 220–288, Ecology Press, Moscow, 1996.

Lazareva, L. I., A. M. Ashadze, B. N. Batuev, and A. R. Nesterov, Concentration mechanisms and forms of gold and silver occurrence in the sulfide ores of the Mir structure and Polyarnoe ore field, Mid-Atlantic Ridge, *Abstracts of Papers: XII International Seminar on Marine Geology, 2,* pp. 161–163, Moscow, 1997.

Lein, A. Yu., Sulfur and carbon isotopes on the active hydrothermal fields of the Mid-Atlantic Ridge, *Russian Journal of Earth Sciences, 2,* (4), 1–12, 2000.

Lein, A. Yu., and A. M. Sagalevich, Rainbow black smokers – a region of extensive abiogenic methane synthesis, *Priroda,* (8), 45–53, 2000.

Lein, A. Yu., V. F. Galchenko, N. V. Ulyanov, et al., The mineral composition and geochemistry of rocks with bacterogenic overgrowths from submarine hydrothermal structures, *Geokhimiya, 9,* 1235–1248, 1988.

Lein, A. Yu., D. V. Grichuk, E. G. Gurvich, and Yu. A. Bogdanov, A new type of hydrothermal hydrogen- and methane-rich solutions in the rift zone of the Mid-Atlantic Ridge, *Doklady Ross. Akad. Nauk, 375,* (3), 380–383, 2000.

Lein, A. Yu., N. V. Ulyanova, V. A. Grinenko, et al., Mineralogy and geochemistry of hydrothermal sulfide ore in the Manus Basin, Bismarck Sea, *Geokhimiya,* (4), 524–538, 1993.

Mozgova, N. N., S. G. Krasnov, Yu. S. Borodaev, et al., The structure, mineral assemblages, and precious metals of the Mir ore structure (Mid-Atlantic Ridge, $26°$ N), *Geol. Rudn. Mestorozhd., 40,* (3), 228–249, 1998.

Petrovskaya, N. V., Native gold, in *Typomorphism of Minerals,* Nedra, Moscow, 1989.

Pimenov, N. V., A. S. Savichev, I. I. Rusanov, et al., Microbiologic processes of carbon and sulfur cycles at cold methane seeps in the North Atlantic, *Microbiologiya, 69,* (6), 810–818, 2000.

Sagalevich, A. M., G. M. Vinogradov, E. G. Gurvich, et al., Surveys at the Titanic Site and Rainbow hydrothermal field during cruise 42 of R/V Akademik Mstislav Keldysh, *Okeanologiya, 40,* (3), 468–475, 2000.

Simonov, V. A., Yu. A. Bogdanov, and I. V. Vikentiev, The physicochemical parameters of the Rainbow hydrothermal ore deposition systems (Mid-Atlantic Ridge), in *Metallogeny of Old and Present-day Oceans–2000,* pp. 110–113, Ural division, Russian Academy of Sciemces, Mias, 2000.

Vikentiev, I. V., N. S. Bortnikov, Yu. A. Bogdanov, et al., Mineralogy of hydrothermal deposits of the Rainbow field in the Azores area (Atlantic), in *Metallogeny of Old and Present-Day Oceans–2000,* pp. 103–109, Ural Division, Russian Academy of Sciences, Mias, 2000.